# PULMONARY TARGETING OF INHALED GLUCOCORTICOID DRY POWDERS

By

JAMES DAVID TALTON

A DISSERTATION PRESENTED TO THE GRADUATE SCHOOL
OF THE UNIVERSITY OF FLORIDA IN PARTIAL FULFILLMENT
OF THE REQUIREMENTS FOR THE DEGREE OF
DOCTOR OF PHILOSOPHY

UNIVERSITY OF FLORIDA

1999

ACKNOWLEDGEMENTS

I would like to extend my appreciation to many people who have helped me through the years. I would first like to thank my advisor, Dr. Guenther Hochhaus, for his support and patience over the last four years. I would like to thank the members of my supervisory committee, Dr. Hartmut Derendorf, Dr. Jeffrey Hughes, and Dr. Gayle Brazeau, for their leadership and friendship. I would especially like to acknowledge my external committee member, Dr. Christopher Batich, for his guidance over the last seven years throughout my undergraduate and graduate research.

I would like to thank the graduate students, staff, and professors in Materials Science and Engineering. Special thanks to: James Fitz-Gerald, James Marotta, Bob Hadba, Chris Widenhouse, Drew Amery, James Kirk, Kaustubh Rau, Paul Martin, Brent Gila, Sean Donovan, Mike Ollinger, Dr. Rajiv Singh, Dr. Eugene Goldberg, Dr. Anthony Brennan, and many others.

I would also like to thank the graduate students, staff, and professors in Pharmaceutics and the College of Pharmacy. Special thanks to: Sandra Suarez, Suliman Al-Fayoumi, Earvin Liang, Jeff Stark, Scott Poxen, Ampara de la Pena, Sriram Krishnasmami, Fuxing Tang, Brett Houk, Intira Coowanitwong, Vikram Arya, Pretti Ajmani, Yufei Tang, Marge Rigby, Pat Khan,

Jim Ketcham, Vada Taylor, and the many exchange students who visited the lab over the years.

In addition I would also like to thank several people who have donated their expertise and equipment to assist me in my research. I would like to thank Dr. Greg Schultz and the Center for Wound Healing for first getting me interested in drug delivery. I would also like to thank the staff of the Major Analytical Instrumentation Center and the Engineering Research Center for Particle Science and Technology for their assistance in sample characterization. Special thanks to Dr. Sue Way and Dr. Shirlynn Chen at Boehringer Ingelheim for their help during my summer internship.

Finally, many thanks to some special family and friends that have been supportive over the years. Special thanks to my mother, father, brother, sister, and family for their love and support during my extended years of education.

TABLE OF CONTENTS

page

KEY TO ABBREVIATIONS

| | |
|---|---|
| BDP | Beclomethasone dipropionate |
| BUD | Budesonide |
| Cl | Clearance |
| DEX | Dexamethasone |
| DPI | Dry-powder inhaler |
| F | Bioavailability |
| FP | Fluticasone propionate |
| fu | fraction unbound |
| GR | Glucocorticoid receptor |
| GRE | Glucocorticoid response element |
| IT | Intratracheal |
| IV | Intravenous |
| LC/MS/MS | Liquid chromatography with double mass spectrometer |
| MAT | Mean absorption time |
| MDI | Metered-dose inhaler |
| MET | Mean effect time |
| MRT | Mean residence time |
| PGA | Poly(glycolic acid) |
| PLA | Poly(lactic acid) |
| PLGA | Poly(lactic-co-glycolic acid) |
| RBA | Receptor binding affinity |
| SPE | Solid phase extraction |
| $T_{1/2}$ | Half-life |
| $T_{50\%}$ | Dissolution half-life |
| TA | Triamcinolone acetonide |
| TAP | Triamcinolone acetonide phosphate |
| TFA | Tri-fluoroacetic acid |
| Vd | Volume of distribution |

Abstract of Dissertation Presented to the Graduate School
of the University of Florida in Partial Fulfillment of the
Requirements for the Degree of Doctor of Philosophy

PULMONARY TARGETING OF INHALED GLUCOCORTICOID
DRY POWDERS

By

James David Talton

August 1999

Chairman: Günther Hochhaus
Major Department: Pharmaceutics

Although new inhaled glucocorticoids introduced for the treatment of asthma in the last decade have been shown to have lower oral bioavailability and higher systemic clearance, systemic side effects are still observed. Although the efficacy of inhaled glucocorticoids is well established, it is difficult to assess their pulmonary targeting (local vs. systemic effects) in humans, mainly because of the lack of appropriate surrogate markers for pulmonary effects. Computer simulations have shown that, based on receptor occupancies in individual organs, pulmonary targeting can be improved by optimization of drug release rate. In addition, it has previously been shown using liposomes that pulmonary targeting is improved by increasing the pulmonary residence time, but the industrial application of liposome formulations are limited.

The overall objective was to compare the dissolution rates *in vitro*, and pharmacokinetics and pulmonary targeting *in vivo* of three currently available

inhaled glucocorticoid dry powders (triamcinolone acetonide, budesonide, and fluticasone propionate) and one sustained release formulation (micro-encapsulated budesonide). First, dissolution of fluticasone propionate was shown to be slower than triamcinolone acetonide and budesonide *in vitro*. *In vivo* experiments in rats showed comparable fast absorption times for budesonide and triamcinolone acetonide and slower absorption for fluticasone propionate. Next, comparison of the pulmonary targeting using an *ex vivo* receptor-binding assay showed fluticasone propionate displayed the highest level of pulmonary targeting followed by triamcinolone acetonide and budesonide. Then, to further evaluate the relationship of dissolution rate on pulmonary targeting, polymeric microencapsulated budesonide was investigated. Although SEM analysis showed that polymer coatings did not substantially increase particle size, the *in vitro* dissolution half-life increased ten-fold. The pharmacokinetic profile *in vivo* showed a slower absorption rate for coated budesonide than free dry powder formulations. Finally, *ex vivo* receptor binding of coated budesonide showed a statistically significant increase in pulmonary targeting when compared to free powders of budesonide and fluticasone propionate. This method of extending the release-rate of the encapsulated material using polymeric-coated particles has promising industrial applications, and further emphasizes the relationship between increasing pulmonary residence time to improve pulmonary targeting.

# CHAPTER 1
# BACKGROUND

## Introduction

To clearly understand the effects of inhaled glucocorticoids used for asthma therapy, the pharmacokinetic and pharmacodynamic factors involved must be evaluated. In this background section the current literature on asthma therapy as it pertains to glucocorticoids, the physical factors of aerosol delivery, and the pharmacokinetic / pharmacodynamic factors are discussed. Also, descriptions of the three currently available glucocorticoids that are evaluated in this thesis are given, namely triamcinolone acetonide (TA), budesonide (BUD), and fluticasone propionate (FP). Finally, a background of the different sustained release mechanisms for pulmonary drug delivery is reviewed.

## Glucocorticoids in Asthma Therapy

Glucocorticoids are used as the first-line treatment in asthma therapy [1]. Systemic administration of glucocorticoids is only recommended if the disease can not be controlled with local therapy. Thus, inhalation therapy is generally applied to achieve high local activity with reduced systemic side effects. There are currently several inhaled glucocorticoids on the market, such as

beclomethasone dipropionate, triamcinolone acetonide, flunisolide, budesonide, and fluticasone propionate.

While there have been numerous review articles describing the clinical efficacy of inhaled glucocorticoids in asthma therapy [2-9], detailed reviews on the underlying pharmacokinetic behaviour and local vs. systemic effects of these drugs are rare. More studies regarding the pharmacokinetic properties of inhaled glucocorticoids and their relationship to the degree of pulmonary targeting or selectivity would be beneficial [4, 10-13].

A pharmacokinetic multi-compartment model is shown in Figure 1.1 (adapted from [14]) that illustrates several of the factors involved in pulmonary drug delivery that will be reviewed in this chapter. Briefly, the aerosol dose is inhaled through the mouth and a portion is deposited in the oropharynx and swallowed (swallowed fraction) or is deposited in the lungs (inhaled fraction). The swallowed fraction, including a portion that is deposited in the upper lung that is subjected to mucociliary transport, is then available to be absorbed in the GI and is subject to the first pass effect in the liver before passing into the systemic compartment (according to its oral bioavailability). The drug particles deposited in the lungs will dissolve according to its dissolution rate $k_{diss}$ and will be available for absorption into the lung tissue (which is generally fast for glucocorticoids). Absorbed drug in the lungs, $C_{lung}$, may then be bound to the pulmonary glucocorticoid receptors (according to the $EC_{50}$) and then absorbed systemically according to its absorption rate $k_{abs}$ (also generally fast). A portion of drug that enters the systemic compartment binds to tissues according to the

volume of distribution and the plasma protein binding. Non-protein bound drug in the plasma is then available to be bound to systemic glucocorticoid receptors (according to the $EC_{50}$). Elimination of drug from the systemic compartment occurs via clearance mainly in the liver. From this model the physical and pharmacokinetic parameters of inhaled glucocorticoids that improve the local vs. systemic effect ratio, or the pulmonary targeting, are a high pulmonary deposition ratio, low oral bioavailability (F), high volume of distribution (Vd), high clearance (Cl), and most importantly a slow pulmonary dissolution or absorption rate (see Table 1.1). These pharmacokinetic factors in humans will be discussed individually in this background chapter.

Table 1.1: Factors important for pulmonary targeting.

| Pulmonary components | Systemic components |
|---|---|
| Pulmonary deposition efficiency | Oral bioavailability |
| Location of pulmonary deposition | Oral deposition efficiency |
| Pulmonary residence time (dissolution rate and other factors) | Clearance |
| | Volume of distribution |
| Pulmonary absorption rate | Tissue distribution pattern |
| Pharmacodynamic drug characteristics in the lung | Pharmacodynamic drug characteristics in systemic tissues |

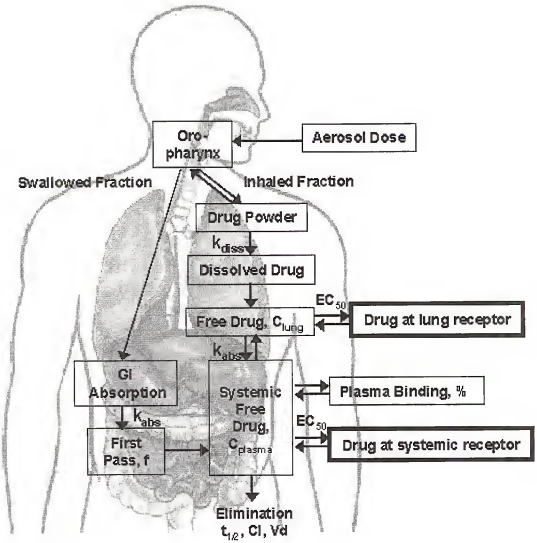


Figure 1.1: Pharmacokinetic multi-compartmental model of inhaled drug delivery.

Glucocorticoid Mode of Action

The glucocorticoid receptor (GR) belongs to the steroid superfamily of cytosolic receptors [15]. In its inactive state the GR is bound by two molecules of 90 kD heat shock protein (HSP-90) and one molecule of the immunophilin p-59, covering the DNA binding region of the receptor [16, 17]. Glucocorticoids

exert their action directly by binding to the intracellular GR and translocating to the nucleus, binding to specific glucocorticoid response elements (GRE) and modulating DNA transcription through several mechanisms (see Figure 1.2, adapted from [18]). Two isoforms of the human GR, hGR-$\alpha$ and hGR-$\beta$, have been identified recently [19], with only the hGR$\alpha$ isoform activated by glucocorticoids. Both isoforms are transcriptionally active, though, with the hGR$\beta$ isoform providing an antagonistic effect to the glucocorticoid-activated hGR$\alpha$ isoform [19].

When the glucocorticoid receptor is activated, it dissociates from the complex with HSP-90 and p-59, exposing a pair of DNA-binding zinc fingers [20]. Two activated GR's must be present to form a homodimer which is then able to interact with specific DNA GREs. Binding of the liganded GR to DNA results in either induction or repression of responsive genes through these GRE's, such as increased mRNA expression for tyrosine aminotransferase (TAT) in the liver [21].

Recent studies have found that the bound GR also modulates gene transcription through indirect protein-protein interactions with transcription factors such as AP-1 (activating protein-1) and NF-K$\beta$ (nuclear factor K$\beta$), which induce many of the inflammatory genes that are abnormally expressed in asthma [22]. These recently discovered indirect pathways are extremely important because they provide a crosstalk between glucocorticoids on one hand, and polypeptide hormones and cytokines on the other. Some of the genes regulated by this pathway include metalloproteinases, such as stromelysin and collagenase, and

many cytokines, such as IL-2 [22]. The repression of these genes is likely to underlie the anti-inflammatory and immunosuppressive effects of glucocorticoid therapy.

Glucocorticoid receptors are distributed throughout the body in many tissues and are essentially the same in humans and other species [8]. Independent of the binding mechanism, the degree of effects and side effects from a glucocorticoid dose is directly related to the number of activated receptors in the cells of a tissue [21]. This suggests that, for both local effects and systemic side effects, the receptor occupancies in local and systemic organs are highly suitable for describing the activity of a glucocorticoid [21]. Although, more potent glucocorticoids with high receptor binding affinities (such as budesonide, beclomethasone monopropionate, and fluticasone propionate) have recently been developed, they are not necessarily more efficacious. More potent glucocorticoids with lower $EC_{50}$ values (effective concentration which binds 50% of the receptors) have corresponding increasing receptor binding affinities (RBA) for systemic glucocorticoid receptors as well in the lung [8]. The relationship of a high receptor binding affinity increasing the extent of local and systemic effects has been demonstrated previously using computer simulations [14].

Asthma

Asthma is an inflammatory disease of the airways associated with mucosecretion, hyperreactivity, epithelial cell injury, and deposition of fibrous material in the subepithelial basement membrane. The physiological changes

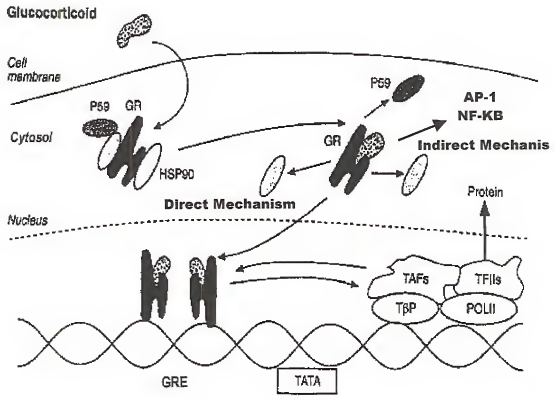


Figure 1.2 Mechanism of glucocorticoid binding to cytosolic glucocorticoid receptor (GR) and translocation to nucleus (adapted from [18]).

that occur in asthma include an increase in the non-specific reactivity of the airways to a variety of bronchospastic agents including histamine, metacholine, adenosine, and leukotrienes [23]. It is unknown if damage in the airway epithelium occurs prior to the inflammatory reaction or as a result of released mediators from inflammatory and mast cells. The interactions between the epithelial cytoskeleton and its transmembrane receptors and the epithelial basement membrane and stroma may play an important role in the pathogenesis of asthma [24].

Many cells are involved in asthma including eosinophils, macrophages, mast cells, epithelial cells, and lymphocytes (see Figure 1.3 adapted from [25]). The interactions of these cells result in the release of different mediators leading to bronchoconstriction, microvascular leakage, mucus hypersecretion, epithelial damage, and stimulation of neural reflex [26]. For example, macrophages produce IL-1 which may prime eosinophils to respond to other secretory stimuli [27]. It has been suggested that the immunosuppressive effects of glucocorticoids can also be mediated via inhibition of NF-Kβ through induced synthesis of the NF-Kβ inhibitory protein IKβ-9 [22]. Similar to this mechanism, glucocorticoids inhibit the transcription of a number of cytokines and chemokines relevant to the pathogenesis of asthma [28].

Cytokine generation in the airways triggers in part infiltration of inflammatory cells into the airways. There are several classes of cytokines involved in allergic cell recruitment including non-specific endothelial activators (TNF-α and IL-1), specific endothelial activators (IL-4 and IL-3), miscellaneous activators (IL-3, IL-5, granulocyte-macrophage colony-stimulating factor (GM-CSF), and interferon gamma), and direct cell migrators (RANTES) [29]. The release of these cytokines has been shown to be modulated by glucocorticoid therapy, thus minimizing mediator release and inflammatory cell migration [30].

Therapy of Asthma

The overall management of asthma involves immediate relief from bronchconstriction (for example with β-agonists) and the control of the

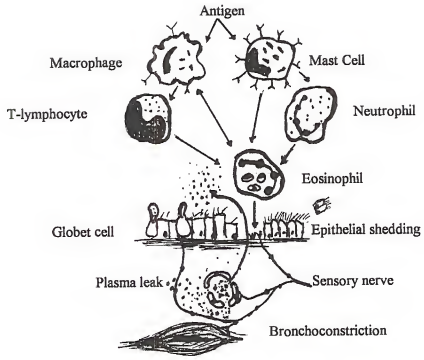


Figure 1.3 Antigen effect on pulmonary cells associated with asthma [25].

inflammatory response (for example with glucocorticoids) [31]. Controlling the allergic response to the local environment, due to smoking and allergens found at home or in the workplace, is the first priority in minimizing asthma hyper-responsivity [31]. Drug therapy for asthma includes five classes of medications: anticholinergics, beta-adrenergic agonists, theophylline, sodium cromolyn glycate, and glucocorticoids [24]. Many controlled trials have now established that inhaled glucocorticoids are the most effective medications because of their

effects at the cellular levels to attenuate the late response and reduce the overall need for beta-agonists [32, 33].

## Physical Factors of Inhaled Glucocorticoid Therapy

Localized delivery of drugs to the lungs has become an increasingly important therapeutic method for treating a variety of diseases including asthma, bronchitis, and cystic fibrosis [34]. The theory behind inhalation therapy for localized delivery is that only relatively small doses are required for effective therapy, reducing exposure of drug to the systemic circulation, and potentially minimizing systemic side-effects [35]. These low dosage regimens may provide considerable cost savings, especially with expensive therapeutic agents. Localized drug delivery directly to the lung should, in theory, maximize therapeutic effect while minimizing unwanted side effects. As mentioned earlier, these advantages are the basis of inhalation therapy of glucocortioids.

### Inhalers

There are a variety of inhalers on the market today with different methods of delivering aerosolized drug to the lung, including metered-dose inhalers (MDI's), dry-powder inhalers (DPI's), and nebulizers. The pulmonary deposition efficiency of the inhaled drugs, or the ratio of dose effectively deposited in the lungs to the dose entering the mouth, can be either determined by gamma scintigraphy or pharmacokinetic techniques [36-38]. The deposition efficiency depends on the physical characteristics of the liquid aerosol or dry

powder particles, the velocity of the aerosolized particles, and breathe coordination [39, 40].

Pulmonary deposition also depends on the nature of the delivery device used. Pulmonary deposition of conventional metered-dose inhalers (MDIs) depends on physicochemical characteristics of the device, such as aerosol size, density, and velocity, as well as by the coordination of inhalation [37]. Pulmonary deposition of MDIs has been generally shown to be in the range of 10-20% [41-43] with significant oropharyngeal deposition because of the exiting aerosol velocity [44]. Moderate increases in pulmonary deposition efficiency of metered dose inhalers has been achieved with the use of spacer devices that slow aerosol velocity [41, 45-49]. Aerosol deposition in the human lung has been also optimized by actuating the aerosol in coordination with breath rate following administration from a microprocessor-controlled pressurized metered-dose inhaler [50, 51]. Improvement in newer MDIs with increases in deposition efficiencies of up to 40% have been reported [52, 53].

Because of the FDA limiting the use of CFC's earlier this decade, dry-powder inhalers have gained much attention. Dry-powder formulations have been characterized by increases in stability, more uniform particle size distributions, and less impaction in the oropharyngeal because the aerosol is not pressurized [54]. Early reports on DPI's suggested similar deposition efficiencies to MDI's (10-20%). Newer dry-powder inhalers have shown high pulmonary deposition efficiencies [55, 56], but show high variabilities across different studies [57]. For DPI's, the deposition efficiency depends on the inspiratory flow of the

patient [58] and dry powder inhalation devices might be unsuitable for patients with very low inspiratory flow.

Common nebulizers use ultrasonic or jet aerosolization of solutions, and although bulky are common in home therapy. Nebulizer efficiency has been tested by Hardy [59] and found to be dependent on the brand and system of nebulizer employed with pulmonary deposition ranging from 2 to 20%. Spacer use generally increases efficiency of jet nebulizers [60]. Newer studies by the same group showed, in general, a higher deposition of ultrasonic nebulizers when compared with jet nebulizers [60]. The use of nebulizers has been recommended for patients with severe bronchoconstriction [61] and in chronic asthma in adults [62], but depends on the aerosol characteristics and output [63].

Generally, the pulmonary selectivity of an inhaled glucocorticoid will increase with increased pulmonary deposition. A high pulmonary deposition will therefore be advantageous. However, the benefits of improved pulmonary deposition are more important for substances with distinct oral bioavailability [14, 64].

Structure and Function of the Respiratory Tract

The respiratory tract can be divided into upper airways, including the mouth, trachea, and larynx, and lower airways, including the bronchi, bronchioles, and alveoli [65]. The lower airways resemble a series of tubes undergoing regular dichotomous branching. Further branching from the bronchi to the alveoli reduces the diameter of the tubes, with marked increases in the surface area of the airways, which allows ease of gas exchange [66]. The lower

airways can be divided into two physiological zones: central and peripheral. The central zone consists of the larger tubes responsible for the bulk movement of air and blood. In the central airways, airflow is rapid and turbulent and less gas exchange occurs. The epithelial layers of the trachea and main bronchi are made up of several cell types including ciliated, basal, and goblet. A large number of mucous- and serum-producing glands are located in the submucosa [66].

The peripheral section of the human lung consists of smaller bronchioles and the alveoli. Each bronchiole ends in many acini, which consists of the alveolar ducts, alveolar sacs, and alveoli. The primary cells of the epithelium in the acini are the type I pneumocytes, which cover 90% of the entire alveolar surface, and type II pneumocytes, which are more numerous but have a smaller total volume and are responsible for the storage and secretion of lung surfactant. Other less prevalent cell types include type III pneumocytes and alveolar macrophages. The alveolar blood barrier consists of a single epithelial cell, a basement membrane, and a single endothelial cell. While this morphological arrangement readily facilitates the exchange of gases and small molecules, it can still represent a major barrier to large molecules [67]. Once dissolved, though, absorption of lipophilic and low molecular weight drugs such as glucocorticoids is fast because the lung tissue is so highly vascularized, similar to the gastrointestinal (GI) tract. Unlike oral delivery of drugs through the GI, inhaled drugs are not subject to changes in pH or first-pass metabolism [34].

Mechanisms of Drug Deposition

As discussed above, drugs for inhalation therapy are administered in aerosol form. From the inhaler, the aerosol is characterized as a suspension of liquid or solid particles dispersed in a gas phase. The main physical parameter for high therapeutic efficacy is the ability of the aerosolized drug to reach the airways of the lungs. The physiology of the human respiratory tract, though, has evolved to prevent the entry of particulate matter. Upon actuation of the inhaler, the deposition efficiency is determined by the ratio of drug that exits the inhaler and the amount that is absorbed through the lung, with the rest either swallowed or redistributed by the mucociliary transport system in the upper bronchi [68].

Particle Characteristics

The particle's geometric and aerodynamic diameter are critical parameters affecting their flow and site of deposition, since these parameters determine the aerodynamic and gravitational mechanisms that affect the extent of penetration into the lungs. Aerosol particle size is expressed in terms of aerodynamic diameter ($D_{ae}$), which is defined as the diameter of a similar spherical particle having unit density (1.0 g/cc) that has the same flow velocity [68]. Thus, larger particles with lower densities will have similar aerodynamic diameters and may yield similar deposition profiles to smaller particles at standard densities [69]. Byron [70] showed that maximum pulmonary deposition occurs with particles between 1 to 5 microns, with particles larger than 5 microns gaining sufficient momentum to impact in the back of the throat, and particles

smaller than 5 microns being breathed back out. Overall the physical factors for maximum aerosol deposition in the lung include (1) aerosol $D_{ae}$ < 5 microns to minimize oropharyngeal deposition, (2) aerosol $D_{ae}$ > 1 micron, and (3) slow, steady inhalation and a period of breath holding on completion of inhalation to minimize exhalation of the drug.

## Pharmacokinetic / Pharmacodynamic Parameters

It is important to understand the underlying pharmacokinetic factors of the inhaled glucocorticoids (deposition ratio, oral bioavailability, absorption, distribution, and clearance) that lead to the local and systemic effects for improving the overall clinical efficacy [4, 10-13]. A pharmacokinetic compartmental model after inhalation is shown in Figure 1.1 and pharmacokinetic parameters for three of the five currently available inhaled glucocorticoids (dexamethasone shown for comparison only) listed in Table 1.2.

Table 1.2: Pharmacokinetic parameters of inhaled glucocorticoids.

| Drug | Abbr | RBA | fu (%) | CL (L/h) | $Vd_{ss}$ (L) | $t_{1/2}$ (h) | $F_{oral}$ (%) |
|---|---|---|---|---|---|---|---|
| Dexamethasone | DEX | 100 | 32 [73] | 17 [77] | 106 [77] | 4.6 [77] | 83 [82] |
| Triamcinolone Acetonide | TA | 361 [72] | 23 [74] | 37 [79] | 103 [79] | 2.0 [79] | 23 [79] |
| Budesonide | BUD | 935 [72] | 12 [75] | 84 [75] | 183 [75] | 2.8 [75] | 11 [75] |
| Fluticasone Propionate | FP | 1800 [72] | 10 [76] | 69 [78] | 318 [78] | 6.0 [78] | <1 [81] |

Oral Bioavailability

Glucocorticoids are inhaled to achieve localized pulmonary effects, but unfortunately much of the inhaled dose is swallowed [14]. Considering the high degree of orally-impacted and swallowed drug (commonly > 50% of the dose), a significant amount of the dose is available for oral absorption. This part of the dose will reduce the pulmonary selectivity of the drug, if orally bioavailable. Thus, the optimal inhaled glucocorticoid should consequently show minimal oral bioavailability. The hepatic clearances of most of the inhaled glucocorticoids are close to the liver blood flow of 90 L/hr, resulting in a high first-pass effect. In particular, fluticasone propionate [82, 83] possesses an extremely low oral bioavailability of close to 0%. It has be shown for fluticasone propionate that high first pass effect and poor absorption from the gastrointestinal tract are responsible for its low oral bioavailability [82, 83]. Slightly higher oral bioavailabilities have been reported for budesonide (11%, [74]) and triamcinolone acetonide (23%, [84]).

Pulmonary Absorption

A slow pulmonary absorption has been classified as a key component for successful targeting of the inhaled glucocorticoids [14]. It is now recognized that an increased pulmonary mean residence time of an inhaled glucocorticoid is not only beneficial for a prolonged activity but also for increased pulmonary targeting [14, 85]. However, obtaining a distinct pulmonary residence time is difficult because of the high surface area and high blood flow.

Comparison of plasma concentrations after inhalation with those obtained after intravenous administration allows the calculation of the mean absorption times. Detailed studies on the pulmonary absorption rate of glucocorticoids have been performed in studies by Schlagel and co-workers [86, 87]. These studies suggest that absorption of aerosolized glucocorticoid solutions from the lung are generally fast, with half-lives of absorption for cortisol, cortisone and dexamethasone of 1.0 to 1.7 minutes [87]. Studies in humans suggest that inhaled glucocorticoids such as flunisolide [88] and budesonide (presumably reaching the lung as solid particles) are also absorbed relatively fast, with maximum plasma concentration times ($t_{max}$) observed after 0.2 [88] and 0.5 hours [55], respectively. Triamcinolone acetonide [89] and fluticasone propionate [90, 91] are absorbed more slowly, though, with $t_{max}$ values of 2.1 hours for triamcinolone acetonide [78] and 1.0 hour for fluticasone propionate [92, 93].

Distribution

The volume of distribution (Vd) is the main pharmacokinetic parameter that describes the plasma protein binding and tissue distribution proportional to the free plasma levels of drug. Although a lower Vd would result in a decrease in half-life of drug (clearance staying the same), a lower Vd only slightly decreases the cumulative systemic side effects. Computer simulations have shown that a short half-life from a smaller volume of distribution is not as substantial a pharmacokinetic factor for improving pulmonary targeting as the clearance [14].

Glucocorticoids are distributed throughout the body extensively because of their high lipophilicity and low molecular weight. Tissue distribution of glucocorticoids is, however, affected by specific glucocorticoid transport systems. Membrane-binding components for cortisol which involve the uptake of corticosteroids into thymocytes [94] and liver cells [95, 96] have been identified. Increased penetration of dexamethasone into the brain has been observed in multi-drug resistance (mdr1A) P-glycoprotein knockout mice when compared to normal mice [97, 98], suggesting that glucocorticoids are substrates for p-glycoprotein efflux.

Unlike the endogenous glucocorticoid cortisol, the currently available inhaled glucocorticoids do not bind significantly to the plasma cortisol transporter transcortin [99]. Rather, α-1 acid glycoprotein [100] and albumin represent the most important plasma protein binding components. Plasma protein binding (see Table 1.2) of the inhaled glucocorticoids ranges from 70-90 % and is roughly related to the lipophilicity of the glucocorticoid. Increases in non-specific binding to tissues also increases with lipophilicity, resulting in increased volume of distributions. The volume of distribution in humans increases such that triamcinolone acetonide < budesonide < fluticasone propionate (see Table 1.2). Although suggested by some investigators [101], increased overall tissue binding does not necessarily increase lung selectivity after inhalation because only free drug concentration and not bound drug is relevant for inducing pharmacological effects.

Interestingly, reversible esterfication of 21-alcohols, such as budesonide, has recently been suggested to increase the pulmonary residence time [102]. Since the fatty acid conjugates are retained intracellularly for a longer time than unchanged budesonide, the duration of tissue exposure to free budesonide depends partly on the rate of lipase-catalyzed hydrolysis of the conjugates [102]. To sustain therapeutic levels, though, a significant portion of the drug would need to be esterified for it to act as an effective depot over time.

Metabolism

Most glucocorticoids are stable in the lung and most other tissues, such as triamcinolone acetonide [103], budesonide [104], and fluticasone propionate [105], with metabolism occurring mainly in the liver by oxidative processes. Relevant oxidative processes include 6-ß-hydroxylation (flunisolide, budesonide, triamcinolone acetonide, fluticasone propionate), 11-oxidation, 6-ketoformation (flunisolide), B-ring dehydrogenation (budesonide, triamcinolone acetonide, flunisolide), 21-oxidation (triamcinlolone acetonide), acetal oxidation (budesonide [106]), A-ring reduction (budesonide), 17ß-side chain cleavage (dexamethasone) and thio-ester cleavage (fluticasone propionate) [107]. Deactivation by cytochrome P450 by hepatic cells and subsequent fast elimination for most of the inhaled glucocorticoids has been reported [85, 104, 107]. Lipophilicity of the glucocorticoid has been shown to enhance the metabolic activity with these enzymes with very lipophilic glucocorticoids showing increased intrinsic clearance (such as fluticasone propionate, [85]).

Clearance

A primary requirement for increased pulmonary selectivity is a high systemic clearance [14, 85]. Figure 1.1 illustrates that high clearance from the systemic compartment will improve pulmonary selectivity by lowering systemic exposure (expressed as the ratio of pulmonary to systemic receptor occupancies). As most of the currently available inhaled glucocorticoids are being inactivated through hepatic metabolism, most inhaled glucocorticoids show systemic clearance values close to the liver blood flow (see Table 1.2) of 90 L/hr. One significant way of improving pulmonary selectivity is to further increase systemic clearance through other mechanisms such as extrahepatic inactivation mechanisms. However, to be a successful inhaled glucocorticoid, such derivatives need to show sufficient pulmonary activity.

Receptor Binding Affinity (RBA)

Receptor binding affinities (RBA) of inhaled glucocorticoids to the glucocorticoid receptor vary significantly (see Table 1.2). Structure-affinity relationships for a variety of synthetic glucocorticoids have shown that the presence of a 1,2 double bond, the existence of a 6 and 9 fluoro or methyl group, and the introduction of lipophilic residues in the 16 and 17 position increase affinity [108-112]. Changes in position 16 and 17 consequently led to the design of more potent inhaled glucocorticoids, such as beclomethasone monopropionate (active species of beclomethasone dipropionate), triamcinolone acetonide, flunisolide, and budesonide, and fluticasone propionate. Glucocorticoids with intrinsic activities 20 times more pronounced than that of dexamethasone have

been described [113]. Interestingly, modifications on the 17ß side chain by adding a thioester of cortienic acid for fluticasone propionate retained glucocorticoid receptor binding affinity [110, 114-116], while introducing a predictable metabolic inactivation group [4]. In contrast, traditional 21-ester of glucocorticoids (such as beclomethasone dipropionate) do not bind to the receptor. As stated earlier, all of the relevant inhaled glucocorticoids bind to the receptor with different potencies.

Pharmacodynamic Effects

A significant body of literature suggests that the receptor binding affinity of a glucocorticoid correlates with its effect at the site of action [14, 21, 117]. Consequently, good correlation's between the receptor binding affinity and the activity in systems not affected by pharmacokinetic properties have been found for a number of pharmacological parameters [118] including topical anti-inflammatory properties [15, 119, 120], activity in skin blanching [116], and modulation of the activity of enzymatic systems such as tyrosine aminotransferase [121]. These *in vitro* assays are useful in providing rankings of relative potencies but, as described previously, many pharmacokinetic factors are involved in obtaining a high local vs. systemic effect.

Studies comparing the receptor binding affinity have failed to compare the clinical efficacies, defined as ratio of dose of drug to therapeutic effect, of the different inhaled glucocorticoids through indirect measurements of asthma severity including full expiratory volume (FEV), peak expiratory flow (PEF), and nonspecific bronchial hyper-responsiveness [8]. Unfortunately, there

is no direct measure of airway inflammation, though, and these measurements are only secondary markers from the pharmacological effect of the inhaled glucocorticoids and show great variability between studies. In addition, surrogate markers of systemic effects in humans such as cortisol suppression and immunosuppression show correlation's to potencies when given in equimolar doses, but little information on pulmonary efficacy [8].

Overall, desired pulmonary effects and deleterious systemic side effects are non-dissociable, with pharmacokinetic properties rather than pharmacodynamic properties important for describing pulmonary selectivity [8]. In fact, theoretical simulations showed that differences in receptor affinity can be overcome by selecting the appropriate dose, assuming larger doses can be inhaled [14]. Thus the pharmacokinetic factors involved in improving the local / systemic effects in pulmonary drug delivery include a high deposition ratio (inhaled fraction / swallowed fraction), low oral bioavailability (F), slow dissolution or absorption rate ($k_{diss}$ or $k_{abs}$), high volume of distribution (Vd), and a high clearance rate (Cl).

## Comparison of Inhaled Glucocorticoids

Currently available inhaled glucocorticoids are based on the 21 carbon atom cortisol structure with four rings, three six-carbon rings and a five-carbon ring. The synthetic anti-inflammatory glucocorticoids are characterized by lipophilic moieties in the 16 and 17 position; $CH_3$, F or Cl moieties in the 6 and 9 positions; and/or double bound carbons in the 1,2 position. Other essential

features include a ketone oxygen at the 3 position, an unsaturated bond between the 4,5 carbons, a hydroxyl group at the 11 position, and a ketone oxygen at the 20 position. By modifying the basic structure of glucocorticoids, it is possible to alter the affinity for the glucocorticoid receptor (GR) and plasma protein binding, modulate the metabolism pathway (oxidation or hydrolytic), and the tissue binding and clearance [122].

Adequate characterization of the overall pharmacokinetic drug properties is a necessary prerequisite for comparing the pulmonary targeting. The time course of the pharmacological response is determined by both the concentration and time of free drug at the receptor site. Therefore to assess the systemic exposure of the drug, it is important to observe the glucocorticoid concentration vs. time profile in the systemic compartment by monitoring the plasma levels. This section summarizes the important pharmacokinetic parameters of three commercially available inhaled glucocorticoids, triamcinolone acetonide (TA), budesonide (BUD), and fluticasone propionate (FP) (see structures in Figure 1.4).

Triamcinolone Acetonide (TA)

Triamcinolone acetonide (TA) entered the asthma market as the Azmacort MDI by Rhone-Poulenc in 1992. Doses of 200 to 400 mcg/day (100 mcg/puff) at 2 to 4 times daily were recently shown to have comparable therapeutic effect in forced expiratory volume [123]. The pulmonary deposition ratio from Azmacort MDI with spacer has been reported to be approximately 22% [73]. First-pass metabolism in the liver to less active metabolites accounts for the

Triamcinolone Acetonide

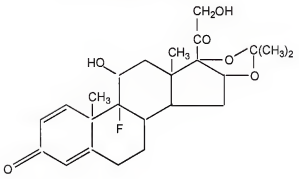


Budesonide

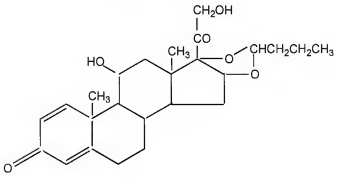


Fluticasone Propionate

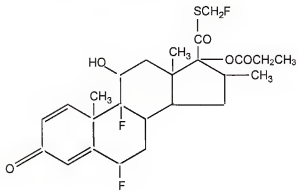


Figure 1.4: Triamcinolone acetonide (TA), budesonide (BUD), and fluticasone propionate (FP) molecular structures.

reduced oral bioavailability of 20 to 25% [78]. Absorption of TA suspension in the lungs has been measured to be approximately 2 hours by the difference in half-lives of intravenous (1.4 to 2.0 hours) versus inhaled (3.6 hours) doses [73, 124].

Triamcinolone acetonide (TA), along with flunisolide, belongs to the second generation of glucocorticoids that show an increased topical potency compared to dexamethasone due to increased receptor binding affinity (RBA = 361) [71]. Plasma protein binding for TA, similar to the other inhaled glucocorticoids, has been reported at 71% [84]. TA has a volume of distribution of 100 to 150 L and has a mean residence time of 2.7 hours after intravenous administration [84, 89, 124]. Clearance of TA is 37.3 L/hr and the major metabolite of TA is 6-hydroxytriamcinolone acetonide, whereas triamcinolone (TC) is only a minor metabolite [89, 124].

Triamcinolone acetonide phosphate (TAP), a water-soluble prodrug which is rapidly metabolized to TA, has been used for IV administration in humans [124]. TAP, which shows dose-dependent kinetics, has a plasma half-life of 3 to 4 minutes and releases active TA immediately. No unchanged ester is found in urine after IV administration, indicating a complete conversion of TAP prodrug to TA. In addition, the total body clearance of TAP exceeds the hepatic blood flow, indicating a large contribution of extrahepatic metabolism due to hydrolysis in the plasma [124]. Previously, our group has shown that pulmonary administration of TAP in a sustained-release liposome formulation resulted in a higher pulmonary residence time, a prolonged pulmonary effect, and a higher lung to systemic drug ratio [125].

Budesonide (BUD)

Budesonide recently entered the US market as Pulmicort Turbohaler (Astra USA) as the first inhaled glucocorticoid dry-powder system. Prescribed doses of 400 to 1,600 mcg per day have been reported [123], with a pulmonary deposition ratio reported of 32% (16 to 59%) for the DPI and 15% (3 to 47%) for the MDI sold in Europe [126]. About 89% of an oral dose of budesonide undergoes first-pass metabolism resulting in an oral bioavailability of 11% [55].

Budesonide has a higher receptor binding affinity (RBA=935) than TA and a higher protein binding (88%) [55]. Its volume of distribution at steady state is 183 L, indicating high tissue affinity. Budesonide is a drug with a very high hepatic extraction ratio and a high clearance (84 L/h) close to hepatic blood flow. The plasma half-life of budesonide is 2.8 hours and is approximately the same after intravenous and inhalation administration, reflecting a fast rate of dissolution and absorption in the lung [74]. Similarly, Thorsson at al. [55] reported a $C_{max}$ of 3.5 nmol/L at 0.3 hour after inhalation via Turbohaler and a $C_{max}$ of 2.3 nmol/L at 0.5 h after inhalation via MDI, indicating dissolution of the dry powder is not rate-limiting.

Budesonide has been shown to have fast dissolution rate in the lung of rats [127] and humans [74]. Thus, decreasing its pulmonary release by encapsulation in microspheres or liposomes is expected to improve the lung selectivity. The lung absorption rate of micronized budesonide in suspension was compared with that of budesonide in solution using isolated perfused rat lungs

[128] with only a marginal difference in lung absorption rate. However, when budesonide 21-palmitate was incorporated into liposomes budesonide showed prolonged retention time (half-life = 6 hr) after intratracheal administration [85]. However, some studies give evidence that a portion of the budesonide dose is retained in lung tissue longer than other steroids because it forms conjugates with long-chain fatty acids (mostly oleic acid) within cells [102]. Such conjugation does not appear to occur with beclomethasone dipropionate, fluticasone propionate or other inhaled glucocorticoids. Budesonide fatty acid conjugates act as an intracellular store of inactive drug since only free budesonide binds to the glucocorticoid receptor. Currently, this depot effect has not been directly correlated to an increase in the therapeutic effect.

Fluticasone Propionate (FP)

Fluticasone propionate (FP) is commercially available as Flovent MDI (Glaxo-Wellcome) and the Diskhaler DPI (Glaxo-Wellcome). Doses of 100-200 mcg/day for children, 200-500 mcg/day for adults with mild asthma, 500-1000 mcg/day for adults with moderate asthma, and 1000-2000 mcg/day for adults with severe asthma are recommended [129]. Following inhalation, 26% of the dose from MDI or 15% of the dose from DPI is deposited in the lung [90], while the majority impacts on the oropharyngeal region and is swallowed. Fluticasone propionate undergoes extensive first-pass metabolism, resulting in a oral bioavailability of less than 1%, and an overall bioavailability after inhalation of 10-15% [83, 130]. Absorption of the lipophilic fluticasone molecule is slow

(MAT of 4.9 hours), leading to prolonged retention in the lungs and lower peak plasma concentrations [131].

Fluticasone propionate has a high RBA of 1,800 and a high plasma protein binding of 90% [Meibohm, 1998] compared to TA and BUD. The volume of distribution of fluticasone propionate at steady state ($Vd_{ss}$) is 318 L, which is in agreement with the high lipophilicity of the molecule [79]. Rapid hepatic clearance of 66 L/hr minimizes systemic side, with almost 87-100% of the drug excreted in the feces, and 3-40% as the inactive 17-carboxylic acid [4].

After IV administration, FP follows a three-compartment body model with its terminal half-life ranging between 7.7 and 8.3 hrs [79]. Absorption of FP in humans is slower than that of TA and BUD and is the overall rate-limiting step in the lungs, and as a result terminal half-life values of 10 hours have been reported after inhalation [93]. In a recent study it was shown that the $t_{½}$ is dose-dependent and ranged between 5.2 and 7.4 hours with a mean of 6.0 ± 0.7 hours [90]. The reported value for the mean residence time of FP after inhaled administration, calculated as the area under the first moment curve (AUMC) divided by AUC, averaged 9.1 ± 1.1 hours (ranging from 7.8 to 11 hours [90]). The mean absorption time after inhalation of FP was found to range from 3.6 to 6.8 hours with a mean of approximately 5.0 hours [90].

## Controlled Release

It has been demonstrated that encapsulation of glucocorticoids into liposomes can lead to the enhancement of therapeutic efficacy, with a reduction

in their toxicity and prolongation of their therapeutic effect [85, 125]. Other methods of obtaining controlled release in the lungs, such as polymeric microspheres and microencapsulation techniques [34], are described in this section.

Liposomes

In the last two decades, it has been demonstrated that encapsulation of drugs into liposomes can lead to the enhancement of therapeutic efficacy, reduction of their toxicity, and prolongation of their therapeutic effect [125]. Liposomes have similar components to natural membranes, composed of phospholipid bilayers entrapping hydrophilic or hydrophobic materials between their aqueous or lipophilic membranes. Through variation in size, lipid composition, charge, number of bilayers and surface characteristics, the release-rate of drug from liposomes and therefore the pharmacokinetics of the encapsulated drug can be modified [67].

Reports of pulmonary delivery of liposomal encapsulated-glucocorticoids are rather scarce. Some glucocorticoids show low encapsulation efficiencies, though, and tend to escape very easily from liposomes, as has been demonstrated for hydrocortisone [132] and for triamcinolone acetonide [133]. In order to overcome this problem different derivatives of glucocorticoids have been used [85, 134, 135]. Encapsulation of triamcinolone acetonide-21-palmitate was shown to have increased liposomal retention of 85%, compared to 5% for the parent drug [134]. Brattsand [85] demonstrated that budesonide 21-palmitate incorporated into liposomes showed prolonged residence time in the lungs of rats

($t_{1/2}$ = 6 hours) compared to free budesonide ($t_{1/2}$ < 2 hours) after intratracheal administration. Recently, pulmonary targeting was enhanced in rats by incorporating triamcinolone acetonide phosphate (TAP) into multi-lamellar liposomes [125]. Overall, these studies suggest that slow release from liposomes induces increased pulmonary targeting, although difficulties in the scale-up manufacturing of liposomes has limited their industrial use [34].

Biodegradable Microspheres

Biodegradable polymers are being used in a large number of biomedical applications such as resorbable sutures, internal fixation devices, degradable scaffolds for tissue regeneration, and matrices for drug delivery. The biocompatibility of these polymers has been reviewed [136]. A variety of synthetic and natural polymers have been found to exhibit minimal inflammatory response in various implantation sites [34].

The advantages of microspheres over liposomes include greater range of sizes, higher stability and shelf life, and longer retention *in vivo* (up to 6 months) [34]. Biodegradation is associated with materials that can be broken down by natural means such as enzymatic or hydrolytic degradation [137]. Biodegradation of poly(lactic acid) (PLA), poly(glycolic acid) (PGA), and their copolymers poly(lactic-co-glycolic acid) (PLGA) yield the natural metabolic products lactic acid and glycolic acid, which are incorporated into the tricarboxylic acid cycle and excreted [69].

Although several reports of inhaled microsphere preparations have shown improvements in targeted and sustained drug release, there have been no

reports on glucocorticoid microspheres. PLGA microspheres of isoproterenol, a beta-agonist bronchodilator, intratracheally administered in rats was shown to ameliorate bronchconstriction for 12 hours in contrast to 30 minutes after free isopreterenol administration [138]. Preparations of large, porous particles of PLGA encapsulated testosterone and insulin by double-emulsion solvent evaporation showed effects up to 96 hours while improving deposition [69]. Sustained release of 2% rifampicin from PLGA microspheres from 3 to 7 days in guinea pigs has been shown reduce mycobacterium infection in macrophages [139]. Unfortunately, low encapsulation efficiencies (<40%) and concerns of accumulation of slowly degrading polymers in the lungs for long-term use have limited the therapeutic application of polymeric pulmonary sustained release systems.

Microencapsulation

The area of microencapsulation is relatively new, previously limited to solvent evaporation techniques [140-143]. Currently there are several different ways of applying coatings to particles in industry, mainly through spray-coating technologies [143]. Pranlukast, a luekotriene inhibiter, encapsulated with hydroxypropylmethylcellulose (HPMC) nanospheres were prepared by spray drying showed an improvement in inhalation efficiency but did not show a significant difference in the dissolution rate [144]. The disadvantages applying micron-thick coatings for sustained-release (10-100 microns thick) [145] is that large quantities of solvents that must be dried under strong venting and that an increase in particle size reduces the inhalation efficiency [34].

A novel coating method has recently been developed using rapid thermal evaporation from a pulsed eximer laser to coat solid materials onto particles [146]. The technique can deposit nanometric coatings (10-1000 nanometers) on core particles ranging from 500 nm to 1000 μm [146]. Through this method, the coating material is generally less than 1% by mass, and coating times are under one hour without the need for drying solvents.

This variation of pulsed laser deposition (PLD) uses high-energy pulses of ultraviolet light to deposit solid coating materials onto particles. Previously there has been a significant emphasis given to control of the particle characteristics (shape, size, surface chemistry, adsorption, etc.), but little attention has been on designing the desirable properties at the particulate surface, which can ultimately lead to enhanced properties of the product [146]. By attaching atomic to nano-sized organic or inorganic, multi-elemental particles either in discrete or continuous form onto the surface of the core particles, that is, *nano-functionalization of the particulate surface*, materials and products with significantly enhanced properties can be obtained.

Only limited reports have used pulsed laser deposition to deposit polymeric nano-particle coatings on flat surfaces [147-150], and none have reported coatings on particles. Through this coating method the coating material is generally less than 1% by mass, and coating times are under one hour without the need for drying solvents. This method has a wide variety of pharmaceutical applications ranging from coatings to improve agglomeration and flowability,

stability, cell uptake and interactions, as well as controlling the release rate of the drug.

## Objectives

Many clinical trials have been performed comparing efficacy of the commercially available glucocorticoids. Unfortunately establishing dose-response studies for comparing clinical effectiveness of the inhaled glucocorticoids has been difficult because of the lack surrogate markers. While glucocorticoids exert many different effects in tissues, the extent of binding to the cytosolic receptors (receptor occupancy) in each organ is presented as a 'universal' surrogate marker from which other local antiinflammatory effects and systemic side effects can be correlated to.

The first objective is to compare the particle size, *in vitro* dissolution, and *in vivo* absorption rate in rats of three inhaled glucocorticoid dry powders, triamcinolone acetonide, budesonide, and fluticasone propionate. As stated above, by comparing the plasma concentrations vs. time the absorption rate can be observed. Then, the relationship of dissolution and absorption rate will be further investigated by comparing the pulmonary targeting in one local (lung) and four systemic (liver, kidney, spleen, and brain) organs of the same three glucocorticoids. For both sets of experiments dry powder formulations will be delivered intratracheally and drug solutions will be delivered intravenously to compare differences in absorption and pulmonary targeting. Then, to further evaluate the dissolution rate and its effect on the absorption rate and pulmonary

targeting, the dissolution rate *in* vitro, absorption rate, and pulmonary targeting *in vivo* of coated budesonide particles will be evaluated.

# CHAPTER 2
# CHARACTERIZATION, *IN VITRO* DISSOLUTION, AND *IN VIVO* PLASMA CONCENTRATIONS IN RATS OF TRIAMCINOLONE ACETONIDE, BUDESONIDE, AND FLUTICASONE PROPIONATE DRY POWDERS

## Introduction

In the past three years there have been two new inhaled glucocorticoids introduced to the U.S., namely fluticasone propionate (GlaxoWellcome) in 1997 and budesonide (Astra) in 1998. These drugs show increased receptor binding affinity, total clearance values approaching the liver blood flow, and as a result low oral bioavailability [74, 129]. Unfortunately, comparing the clinical efficacy and pulmonary targeting of these drugs to traditional inhaled glucocorticoids such as triamcinolone acetonide has been difficult because of the lack of surrogate markers in humans [8].

As discussed previously, our group developed an *ex vivo* receptor binding assay in rats that links a longer release rate of liposomal encapsulated of triamcinolone acetonide phosphate (compared to free drug solutions) with an increase in pulmonary targeting [151]. This relationship is now further evaluated by investigating the *in vitro* dissolution rates and the *in vivo* absorption rates of three different inhaled glucocorticoid dry powders, triamcinolone acetonide, budesonide and fluticasone propionate. Comparisons of the dissolution and

absorption rates observed in this chapter can then be further analyzed by measuring the pulmonary targeting in Chapter 3.

Micronized powders of triamcinolone acetonide, budesonide, and fluticasone propionate were used for these studies. Scanning electron microscopy was performed to ensure particle sizes were homogenous. Then, to evaluate the effect of dissolution rate on the pharmacokinetics, the *in vitro* dissolution of dry powder formulations was performed in a phosphate buffer solution with surfactant at physiological temperature and pH. Because this *in vitro* model utilizes a large volume of buffer and surfactant compared to *in vivo* conditions, this method is used primarily to observe the trend of dissolution rates of the three glucocorticoids.

To analyze the pharmacokinetics of triamcinolone acetonide, budesonide, and fluticasone propionate in rats, plasma concentrations were analyzed after administering equivalent doses *in vivo* in rats. The plasma concentrations were measured by extracting drug from the plasma samples using solid phase extraction (SPE) and injecting into a high-performance liquid chromatography with double mass-spectrometer (LC/MS/MS) system. Overall, the objective of the present study was to compare the particle size, dissolution rates *in vitro,* and pharmacokinetic profiles of triamcinolone acetonide, budesonide, and fluticasone propionate following intratracheal and intravenous administration *in vivo* in rats at equal doses (100 μg/kg rat).

## Hypothesis

Glucocorticoid powders of similar particle size with a slower dissolution rate *in vitro* should display a slower absorption rate *in vivo*.

## Materials and Methods

### Chemicals

Analytical grade chemicals were obtained from Sigma Chemical Co. (St. Louis, MO.). Micronized triamcinolone acetonide was obtained from Sigma. Micronized budesonide was obtained from Sicor (Milan, Italy). Micronized fluticasone propionate was obtained from Glaxo-Wellcome (Research Triangle Park, NC). Micronized fluticasone propionate internal standard, $^{13}C_3$-FP (I.S.), was kindly provided by Glaxo Group Research (Herts, UK). Lactose monohydrate NF extra-fine (particle size 10-30 microns) was obtained from EM Industries (Hawthorne, NY). All other reagents were of analytical grade.

### SEM Analysis

Micronized dry powders were analyzed using a Joel model 6400 EDS scanning electron microscope (SEM) to obtain information on the size, shape, and surface morphology. Micrographs of powder samples were prepared by applying a thin layer of carbon paint onto a graphite sample mount and spreading approximately one milligram on top. Sample mounts then underwent a carbon evaporation process prior to characterization. Characterization was

performed at 1-2 kEV in vacuum. Magnification of representative micrographs was x 5,500.

*In Vitro* Dissolution

*In vitro* dissolution of dry powder formulations (500 mg of 2% drug in lactose) was tested using a USP dissolution bath (VanKel Technology Group, Cary, NC) in 900 ml of pH 7.4 phosphate-buffered saline (50 mM) at 37°C. In order to assure that the powders dissolved completely (FP aqueous sol. 100 ng/ml vs. 90 μg/ml with surfactant), 2% sodium-dodecyl sulfate was added to increase solubility and wetting and to more closely mimic pulmonary surfactant levels *in vivo* [152]. After drug was added one-milliliter samples were removed and filtered through a 0.2 μm syringe filter at 0, 0.5, 1, 1.5, 2, 2.5, 5, 10, 15, 30, 45, 60, and 600 minutes and analyzed using HPLC. Steady-state was reached (10 μg/ml) at 60 minutes (observed from release profiles) and replaced as 100% dissolved.

Glucocorticoid concentrations in solution were analyzed using an HPLC setup consisting of a Perkin Elmer series 3B pump with a flow rate of 1.0 ml/min and a Zorbax C-18 (150 x 4.6 mm) column connected to a Perkin Elmer ISS 100 autoinjector. The detector was a Milton Roy SM-4000 attached to a Hewlett Packard HP-3394A integrator. The eluent was monitored at 254 nm. The mobile phase consisted of a mixture of 40%:60% v/v acetonitrile : 0.03% triflouroacetic acid buffer for TA and 50%:50% v/v acetonitrile : 0.03% triflouroacetic acid buffer for BUD and FP (see Figure 2.1). Samples were injected after standards (5 standards of 1, 5, 10, 50, and 100 μg/ml) for each data

set. Slopes from the calibration curve from standards were used to calculate the sample concentration for each data set ($r^2$>0.99).

Half-life of dissolution was calculated by curve fitting using SCIENTIST program and using the monoexponential formula:

$$\text{Cumulative \% Dissolved} = 100 - [\, A * \exp^{-\alpha t} \,] \qquad \text{(eq. 2.1)}$$

to obtain the dissolution rate constant ($\alpha$). Half-lives of dissolution ($T_{50\%}$) were calculated as $0.693/\alpha$.

Differences in dissolution between drug formulations were tested for significance using the FDA scale-up and postapproval changes (SUPAC) similarity test ($f_2$):

$$f_2 = 50 \text{ x LOG } \{[1+1/n \, \Sigma(R_t-T_t)^2]^{-0.5} \text{ x } 100\} \qquad \text{(eq. 2.2)}$$

where n=13 time points (0, 0.5, 1, 1.5, 2, 2.5, 5, 10, 15, 30, 45, 60, and 600 minutes), $R_t$ = the reference % drug dissolved at time t, and $T_t$. = the test % drug dissolved at time t. An $f_2$ value between 50 and 100 suggests the two dissolution profiles are similar and an $f_2$ value less than 50 indicates a lack of similarity [153].

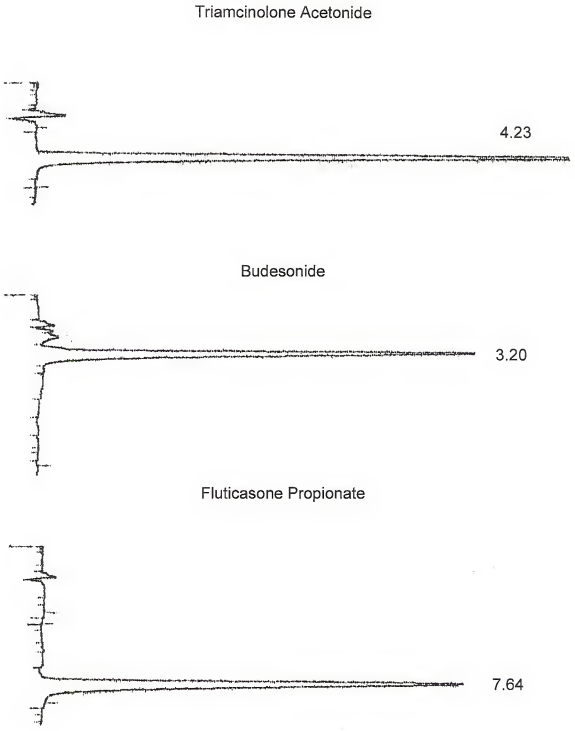


Figure 2.1: HPLC chromatagrams of 100 μg/ml standards of: A) TA, B) BUD, and C) FP

IT Administration in Rats

The Animal Care Committee of the University of Florida, an AAALAC approved facility, approved all animal procedures. Specific-pathogen-free male F-344 rats, weighing approximately 220 to 250 grams, were housed in a 12 hr light/dark cycle / constant temperature environment. Animals were allowed free access to water and rat chow, but were food-fasted overnight prior to each experiment.

On the day of the experiment rats were handled gently to produce minimum stress. Once weighed, the rats were placed in a rat holder for intraperitoneal administration of the anesthetic (fresh preparation of the combination of 1.5 ml of ketamine 10%, 1.5 ml of xylazine 2% and 0.5 ml of acepromazine 1%) at the dose of 1 ml/kg. The depth of anesthesia was checked by tail pinch or pedal withdrawal reflex.

The neck of the completely anesthetized animal was shaved and aseptically cleaned with isopropyl alcohol 70%. A one-centimeter midline vertical incision was made originating above the sternal notch. The neck muscles and glands were carefully dissected midline, until the trachea was exposed and a tracheotomy was performed between the third and fourth tracheal rings. One inch of a 14 gauge Novalon catheter sheath attached to a delivery device for intratracheal (IT) administration of dry powders (Penn-Century, Philadelphia, PA), was introduced into the trachea. A mixture of $5 \pm 0.5$ mg (calibrated with lactose, n=16) of extra fine monohydrate lactose and TA, BUD, or FP (0.4%, 100 $\mu$g/kg dose) was placed in the chamber of the device and instilled in the lungs with

insufflation of 3 ml of air. A sham rat was included in each set of experiments that received 5 mg of the vehicle (lactose). Animals (one animal per time point) including sham rat, were decapitated at 0.5, 1, 2, 4, 6, or 12 hours after instillation. Plasma was snap frozen and stored at -70° C until processing. Organs were processed as discussed in Chapter 3 for receptor binding. Plasma samples for three to five independent experiments using TA, BUD, and FP were performed for a given time point after IT administration.

IV Administration in Rats

For the intravenous (IV) injection of budesonide, animals were anesthetized as described above and the intracardial approach was used. For this approach, IV solution was injected after needle placement in the heart and verified by aspiration of blood. Either 100μl of IV solution (200μg/ml drug) or 100μl of the vehicle (for the sham rat) was injected using a tuberculin syringe with a 27-gauge needle. Animals (one animal per time point) including sham rat, were decapitated at ½, 1, 2, 4, 6, or 12 hours after instillation. Plasma was snap frozen and stored at -70°C until processing. Organs were processed as discussed in Chapter 3 for receptor binding. Plasma samples for three independent experiments for BUD were performed for a given time point after IV administration.

Solid Phase Extraction of Plasma Samples

Frozen plasma samples were thawed at room temperature. A volume of 200 μl plasma was added to 1.8 ml of 10% ethanol with 10 ng/ml final concentration of internal standard ($^{13}C_3$-FP for FP analysis, BUD for TA analysis,

and TA for BUD analysis). Recovery from the extraction technique was measured by spiking blank plasma with 10 ng/ml final concentration of TA, BUD, and FP standard for each sample set. Solid phase extraction (SPE) of compounds was performed as previously described with modifications [154][Li, 1997 #8]. Briefly, samples with 10% ethanol were refrigerated for 15 minutes to precipitate proteins and centrifuged at 4000 rpm. Supernatants were then extracted using ethanol-activated 6 ml endcapped C-18 cartridges (Supelco). The analytes were eluted with 2 x 1 ml of 60% ethyl acetate in heptane. The residue was evaporated under vacuum and reconstituted in 100 μl of methanol-water (80:20, v/v) mobile phase. A total sample volume of 80 μl was injected into the LC/MS/MS system.

LC/MS/MS of Extracted Plasma Samples

The analysis of TA, BUD, and FP was performed as described previously for FP with modifications [155]. A Micromass Quattro-LC-Z (Beverly, MA) triple quadrupole mass spectrometer equipped with an atmospheric pressure chemical ionization (APCI) ion source was used for analysis. The APCI probe temperature was set to 500°C and corona and cone voltages were set at optimum conditions after tuning. The MS/MS signals were optimized by injecting a 1 μg/ml standard in methanol at a flow-rate of 100 μl/min using a Kd-Scientific® infusion pump. At low collision energy, mass analysis was collected through the second quadrople for 432.0>432.0 for TA, 428.0>428.0 for BUD, and 500.0>500.0 for FP. Argon was used as the collision gas at $1.5 \times 10^{-3}$ mBar. The mass spectrometer was linked to a Perkin Elmer ISS-200 autosampler via

contact closure and the operation was controlled by computer software, Masslynx 3.1. The mobile phase was a mixture of methanol-water (80:20, v/v) delivered at a flow-rate of 1.2 ml/min by a LDC/ Milton Roy CM4000 multiple-solvent pump. Chromatographic separations were achieved using a Waters 5-μm ODS2 (4.6 x 50 mm) column (Milford, MA) preceded by a Whatman 5-μm ODS C–18 guard column cartridge (Clifton, NJ). Data analysis was performed using Masslynx software. Samples were injected with calibration curves (4 standards of 1, 10, 20, and 100 ng/ml) for each data set (see Figure 2.2). Slopes from concentration vs. peak area profiles were used for each data set ($r^2$>0.97) and plasma concentrations calculated by multiplying by (Area / Slope) * 2 / Recovery. Recovery percentages, calculated by comparing extracted plasma samples spiked with 10 ng/ml final concentration of TA, BUD, and FP to standards, were calculated as 56.3 ± 5.6% for TA (n=3), 64.1 ± 3.2% for BUD (n=12), and 86.9 ± 3.9% for FP (n=3).

Non-Compartmental Pharmacokinetic Analysis

The non-compartmental analysis for plasma concentrations over time was performed using standard techniques [156]. The time to peak $t_{max}$ (at $C_{max}$) and $C_{max}$ was determined as the highest plasma concentration from the average plasma concentration vs. time profile.

Mean residence time (MRT) for plasma data was calculated from the relationship:

$$MRT_{0\rightarrow\infty} = AUMC_{0\rightarrow\infty} / AUC_{0\rightarrow\infty} \qquad \text{(eq. 2.3)}$$

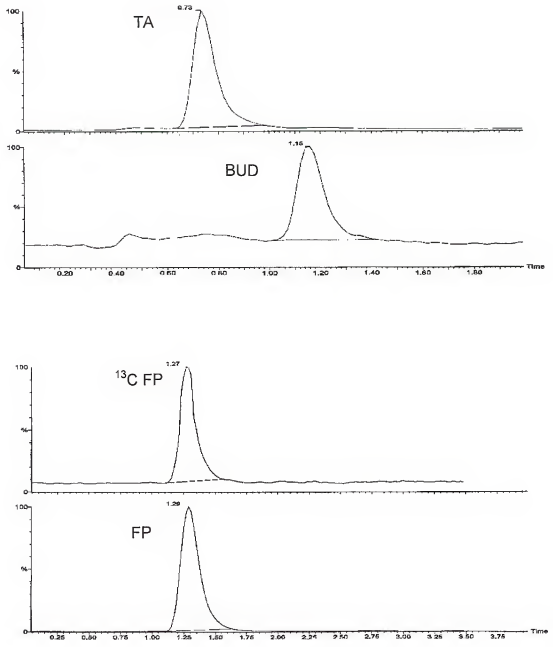


Figure 2.2: LC/MS/MS chromatograms of TA (432>432), BUD (429>429), $^{13}$C FP (503>503), FP (500>500)

where $AUMC_{0\rightarrow\infty}$ is the area under the first moment curve, and $AUC_{0\rightarrow\infty}$ is the area under the curve. The area under the curve ($AUC_{0\rightarrow\infty}$) was calculated by the trapezoidal rule from the C versus time curve ($AUC_{0\rightarrow12}$) and extrapolation to infinity ($AUC_{12\rightarrow\infty}$) calculated by adding the ratio of the last measured $C_{12}$ and the first-order rate constant of the terminal phase ($k_e$, exponential regression from 4 to 12 hours, $r^2$>0.97). The AUC after IV administration was calculated by interpolating $t_0$ from the slope of the first 3 time points (0.5 to 2 hours). The area under the first moment curve ($AUMC_{0\rightarrow\infty}$) was calculated from the C * t versus time curve ($AUMC_{0\rightarrow12}$) and extrapolation to infinity ($AUMC_{12\rightarrow\infty}$) calculated by adding the ratio of the last measured $C_{12}$ * t and the squared of the rate constant of elimination ($C_{12}*t/k_e + C_{12}/k_e^2$).

Differences in AUC's between IV and IT administration were tested for significance using unpaired Student's T-test. Pulmonary bioavailability for clearance determinations (Cl/F) was approximated as 1.0 because the total dose was delivered directly to the lungs. The total body clearance (Cl/F) was calculated as dose divided by $AUC_{0\rightarrow\infty}$ divided by bioavailability (Dose/AUC).

Mean absorption times for TA and BUD plasma data were calculated from the relationship:

$$MAT = MRT_{IT} - MRT_{IV} \qquad \text{(eq. 2.3)}$$

For TA IV, the plasma concentration profile for TAP-sol was used from a previous study [151] based on the assumption that TAP conversion time to TA is negligible

[124] and glucocorticoids in solution are rapidly absorbed into the systemic circulation upon intratracheal instillation [157].

## Results

### SEM Analysis

SEM photomicrographs of micronized dry powders are depicted in Figure 2.3. SEM analysis revealed little difference in particle size and morphology between TA, BUD, and FP from different sources. TA powders displayed some spherical particulates > 3 microns, but were otherwise homogenous. BUD and FP powders were slightly agglomerated but particle sizes were more monodisperse. A quantitative analysis of TA, BUD, and FP particles was not performed, but particle sizes ranged generally from 1 to 3 microns.

### *In Vitro* Dissolution

Cumulative dissolution profiles for TA, BUD, and FP powders are depicted in Figure 2.4. Fitted monoexponential curves showed some divergence from 5 to 10 minutes, but resulting fits showed good correlation ($r^2$>0.99 for all three). Dissolution half-lives of release ($t_{50\%}$ ) were not statistically different for TA and BUD ($f_2$=74), calculated as 1.1 ± 0.1 minutes (n=3) and 1.2 ± 0.1 minutes (n=6), respectively. Dissolution half-life for FP (n=3) was significantly longer than TA ($f_2$=33) and BUD ($f_2$=34) at 4.0 ± 0.4 minutes.

A

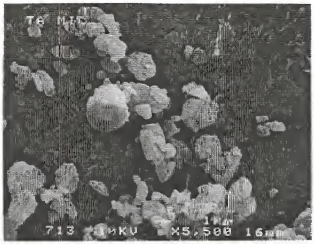


B

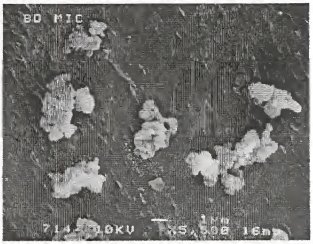


C

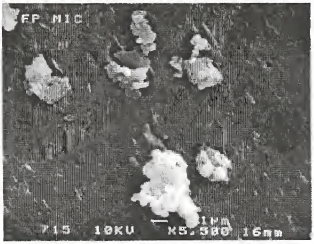


Figure 2.3: SEM micrographs of: A) micronized TA powder, B) micronized BUD powder, and C) micronized FP powder. Resolution 5,500 times magnification.

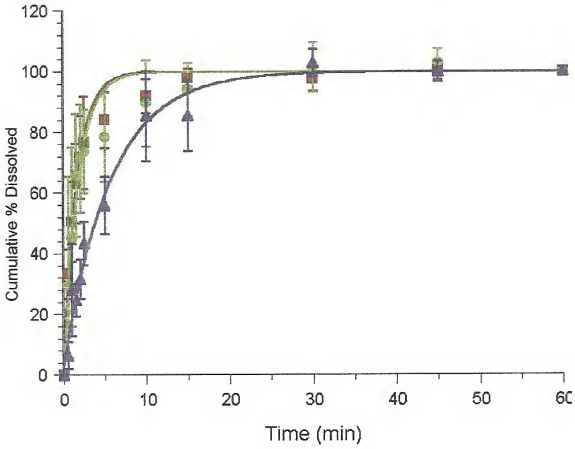


Figure 2.4: Dissolution of triamcinolone acetonide ■ (TA), budesonide ● (BUD), and fluticasone propionate ▲ (FP) dry powders in pH 7.4 PBS (50 mM, 2.0 % SDS) at 37°C (n=3).

Pharmacokinetics of TA in Rats

The average triamcinolone acetonide (TA) plasma concentrations after IT administration of TAP-sol (n=3) and TA dry powder (n=3) are shown in Figure 2.5. The pharmacokinetic parameters resulting from the analysis of plasma data are listed in Table 2.1. The plasma concentrations of triamcinolone acetonide after intratracheal delivery of triamcinolone acetonide phosphate solution (TAP-sol) in rats was previously investigated [151]. TAP-sol was compared to TA dry powder in place of IV data because it has been shown that metabolism of TAP is fast *in vivo* [124] and absorption of glucocorticoids in solution after IT administration occurs relatively unhindered [87].

The maximum TA plasma concentration of 62 ng/ml was observed after the first time point of 1.0 hour for TAP-sol and 200 ng/ml after the first time point of 0.5 hour for TA dry powder. The terminal slope ($k_e$) was 0.6 $hr^{-1}$ for TAP-sol and 0.35 $hr^{-1}$ ($r^2$=0.99) for TA dry powder. The $AUC_{0\rightarrow\infty}$ for the drug plasma concentration-time profiles was 179 ng/ml*hr for TAP-sol and 234 ± 15.9 ng/ml*hr. The clearance (Cl/F) was calculated as 112 ml/hr for TAP-sol and 85.5 ml/hr for TA dry powder. The mean residence time (MRT) was calculated as 1.8 hours for TAP-sol and 2.0 for TA dry powder, with a resulting mean absorption time (MAT) of 0.2 hours for TA dry powder.

Pharmacokinetics of BUD in Rats

The average budesonide (BUD) plasma concentrations after IV administration (n=3) and IT administration (n=5) are shown in Figure 2.6. The

pharmacokinetic parameters resulting from the analysis of plasma data are listed in Table 2.1.

The maximum BUD plasma concentration of 29.3 ng/ml was observed after the first time point of 0.5 hour after IV administration and 48.1 ng/ml after the first time point of 0.5 hour for IT administration. The terminal slope ($k_e$) was 0.26 $hr^{-1}$ ($r^2$=0.99) after IV administration and 0.35 $hr^{-1}$ ($r^2$=0.99) after IT administration. The $AUC_{0\rightarrow\infty}$ was 60.6 ± 26.9 ng/ml*hr after IV administration compared to 85.3 ± 41.2 ng/ml*hr after IT administration, and were not statistically different (p>0.2). The clearance (Cl/F) was calculated as 330 ml/hr after IV administration and 234 ml/hr after IT administration. The mean residence time (MRT) was calculated as 2.4 hours after IV administration and 2.7 after IT administration, with a resulting mean absorption time (MAT) of 0.3 hours after IT administration.

Pharmacokinetics of FP in Rats

The average fluticasone propionate (FP) plasma concentrations after IT administration (n=3) are shown in Figure 2.7. The pharmacokinetic parameters resulting from the analysis of plasma data are listed in Table 2.1.

The maximum FP plasma concentration of 15.2 ng/ml was observed after 1.0 hour after IT administration. The terminal slope ($k_e$) was 0.22 $hr^{-1}$ ($r^2$=0.98) after IT administration. The $AUC_{0\rightarrow\infty}$ for the drug plasma concentration-time profile was 92.0 ng/ml*hr after IT administration. The clearance (Cl/F) was calculated as 217 ml/hr after IT administration. The mean residence time (MRT) was calculated as 5.6 hours after IT administration.

Table 2.1 Pharmacokinetic parameters for BUD TA, BUD, and FP.

| | TAP-sol* | TA IT | BUD IV | BUD IT | FP IT |
|---|---|---|---|---|---|
| $C_{max}$ (ng/ml) | 62 | 200 | 29.3 | 48.1 | 15.2 |
| $t_{max}$ (hr) | 1.0 | 0.5 | 0.5 | 0.5 | 1.0 |
| $k_e$ ($hr^{-1}$) | 0.6 | 0.35 | 0.33 | 0.26 | 0.22 |
| AUC (ng/ml*hr) | 179 | 234 ± 15.9 | 60.6 ± 26.9 | 85.3 ± 41.2 | 92.0 ± 54.5 |
| Cl/F (ml/hr) | 112 | 85.5 | 330 | 234 | 217 |
| MRT (hr) | 1.8 | 2.0 | 2.4 | 2.7 | 5.6 |
| MAT (hr) | | 0.2 | | 0.3 | |

* previously reported from [151].

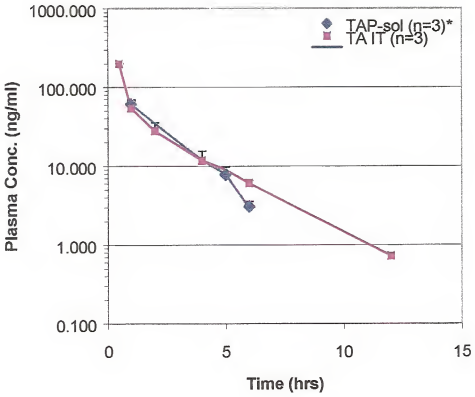


Figure 2.5. Average plasma concentrations (mean + SD) of TAP-sol (n=3*) and TA dry powder (n=3) after intratracheal administration.

* previously reported from [151].

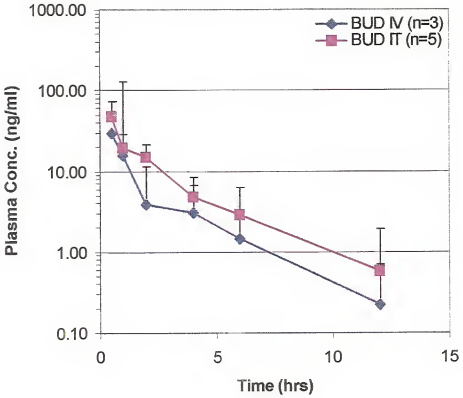


Figure 2.6. Average plasma concentrations (mean + SD) of BUD after intravenous (n=3) and intratracheal administration (n=5).

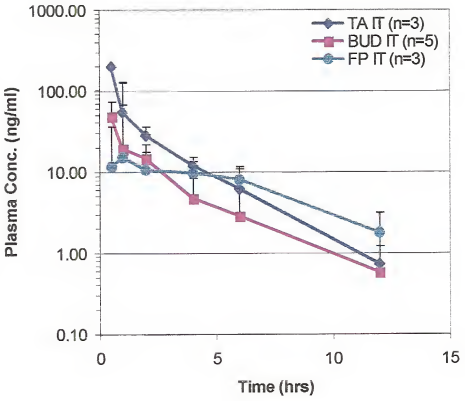


Figure 2.7. Average plasma concentrations (mean + SD) of TA (n=3), BUD (n=5), and FP (n=3) after intratracheal administration.

## Discussion

In the present study we investigated the particle size and morphology, *in vitro* dissolution, and *in vivo* systemic plasma concentrations of triamcinolone acetonide (TA), budesonide (BUD), and fluticasone propionate (FP) after intratracheal (IT) and intravenous (IV) administration. Unfortunately budesonide was the only drug that plasma samples were obtained for after intravenous administration, but aided in comparing absorption of free budesonide powders to the coated powders in Chapter 4. Triamcinolone acetonide phosphate solution delivered intratracheally previously analyzed [151] was substituted for TA IV because, as stated before, absorption of glucocorticoids in solution after IT administration occurs relatively unhindered [87].

The comparison of particle size and morphology using SEM was qualitative rather than quantitative, but verification of particle sizes was necessary to ensure that they were homogenous. Mean particle size was estimated as 1 to 3 microns for all three drugs, which is similar to the particle size used in dry-powder formulations in humans.

Comparison of the dissolution rates of all three powders showed FP had the slowest dissolution half-life of approximately four minutes, with TA and BUD dissolution half-lives close to a minute. While the USP dissolution setup is typically used for monitoring tablet disintegration, this model needs improvement to more closely mimic pulmonary conditions. SDS was used as a surfactant, but the use of human lung surfactant has been studied visually *in vitro* on glass

slides for the inhaled glucocorticoids and produced a similar order in dissolution times comparing BUD (6 minutes) and FP (< 8 hours) [12].

The plasma concentrations of TA after IT administration of TAP solution and TA dry powder were similar at the observed time points from 1 to 6 hours, which indicates that relative bioavailabiltities were similar. Plasma concentrations of BUD after intravenous and intratracheal administration were also similar, which indicates that relative bioavailabilities of BUD were also similar. The AUC for intravenous administration of BUD of 60.6 ng/ml*hr also agrees well with previously reported studies in rats by Chanoine [127] of IV administration of BUD (68 ng/ml*hr). Chanoine also found similar fast absorption of BUD after intratracheal administration with <10% remaining in the lung after 0.5 hour [127]. Plasma concentrations of FP appeared lower after IT administration than TA and BUD, but with a flatter terminal slope. Compartmental analysis was not performed because of the lack of early time points, where a clearer absorption profile should be observable if sampled more frequently. This data was necessary for comparison, though, to the coated particles in Chapter 4.

Comparison of the clearance values (Cl/F) at equal doses (100 μg/kg) were calculated as TA the lowest (85.5-112 ml/hr), FP in the middle (217 ml/hr), and BUD slightly higher (234-433 ml/hr). This trend (TA<FP<BUD), similar to the order of clearance values in humans, is lower than a reported liver blood flow in rats of similar size (250 grams) of 828 ml/hr [158]. The calculated clearance of budesonide in rats was comparable to a previously reported value of

375 ml/hr found by Chanoine after IV administration [127]. The order of calculated clearance values in rats is similar to the trend of clearances in humans of TA being the lowest (37.3 L/hr, [78]), FP in the middle (66 L/hr, [79]), and BUD being the highest (84 L/hr, [74]). Although these values in humans are closer to the liver blood flow of 90 L/hr [158] possibly due to differences in liver enzyme activity or size scaling, the relative rankings are similar.

The mean absorption time (MAT) of TA dry powder was relatively short (MAT=0.2 hour), calculated by the small difference in mean residence times after IT administration of TAP-solution (MRT=1.8 hours) and dry-powder formulation (MRT=2.0 hours). This agrees well with the trend of fast dissolution *in vitro* but not with reported mean absorption time values in humans of 2.9 hours [129], which may be due a slower dissolving formulation in the MDI. Also, the mean absorption time of BUD powders was short (MAT=0.3 hour), calculated by the small difference in mean residence times after IV (MRT=2.4 hours) and IT (MRT=2.7 hours) administration. This agrees well with the fast *in vitro* dissolution and with reported values of fast *in vivo* absorption rates in rats [127] and in humans [129]. Although IV data for FP in rats was not available, the flatter plasma concentration profile of FP showed a later $t_{max}$ at 1.0 hour and the highest MRT of 5.6 hours. This suggests that absorption of FP is slower than TA and BUD, which may be linked to slower dissolution similar to observed *in vitro* results. This also agrees well with the reported $t_{max}$ of FP after inhalation of different doses in humans of 1.0 hour and a high MRT of 9.0 hours [90].

In conclusion, the *in vitro* dissolution of TA and BUD powders was faster when compared to FP powders, which correlated to a faster absorption time for TA and BUD than FP *in vivo*. Overall, the rankings of calculated absorption rates and clearance values for TA, BUD, and FP suggests that similar trends in rankings of absorption and clearance exist between these studies in rats and in published human studies. As previously shown in computer simulations, theoretically glucocorticoids with fast dissolution rates, such as TA and BUD, rapidly enter pulmonary cells but are removed immediately to the systemic circulation and low pulmonary targeting is observed. On the other hand, glucocorticoids with slower dissolution rates, such as FP, obtain higher targeting because drug concentrations in the lung are higher than systemic levels over an extended period of time [14]. To experimentally compare drugs with different dissolution rates and the level of pulmonary targeting the same three drugs (TA, BUD, and FP) will be compared using an *ex vivo* receptor binding assay in rats in Chapter 3.

## Conclusions

- Using SEM analysis, the particle sizes of micronized TA, BUD, and FP powders appeared to be similar (1-3 microns).
- The dissolution of TA and BUD *in vitro* was fast ($t_{50\%}$ < 2 min.), with FP dissolution being slower ($t_{50\%}$ = 4 min.).
- Calculated clearance values for TA, BUD, and FP in rats showed a similar order to calculated values in human studies.

- Absorption *in vivo* of TA and BUD appeared faster and FP, showing a similar trend to dissolution results.

# CHAPTER 3
# ASSESSMENT OF PULMONARY TARGETING OF TRIAMCINOLONE ACETONIDE, BUDESONIDE, AND FLUTICASONE PROPIONATE USING AN *EX VIVO* RECEPTOR BINDING ASSAY

## Introduction

Computer simulations have shown that a higher pulmonary selectivity can be achieved at slower dissolution or release rates, therefore increasing the pulmonary residence time [14]. In addition, the limited data available for currently available inhaled glucocorticoids suggests that drugs with slower dissolution rates, such as fluticasone propionate, have higher pulmonary targeting [159]. Based on these findings it is predicted that drugs with slower dissolution and pulmonary absorption will have increased pulmonary targeting, and conversely that drugs with fast dissolution and absorption rates will show similar profiles in receptor occupancies in local and systemic organs.

The proposed method of investigating this hypothesis was to evaluate the pulmonary targeting (PT) *in vivo* of triamcinolone acetonide, budesonide, and fluticasone propionate administered intratracheally in dry powder lactose formulations and intravenously in IV solutions. These *in vivo* studies will utilize an *ex vivo* animal model previously described [160]. Monitoring the receptor binding in local and systemic organs should provide a more complete profile of the pulmonary targeting. Intratracheal (IT)

administration to the site of action will be compared to intravenous (IV) administration to observe differences in pulmonary targeting after pulmonary absorption. Pulmonary targeting of intravenous administration of TA was previously investigated only in the lung vs. liver receptor binding profiles, which are used for comparison [160]. While these and other studies involving liposomal delivery monitored only receptor binding in the liver to assess the extent of systemic effects, kidney, spleen, and brain were included in this study as systemic organs to further investigate the distribution of the drug throughout the body. Overall, the objective of this section is to compare the pulmonary targeting of TA, BUD, and FP in rats by monitoring the decrease in % free receptors (receptor occupancy) in one local and four systemic organs.

## Hypothesis

Glucocortioid powders with slower dissolution *in vitro* should display higher pulmonary targeting *in vivo*.

## Materials and Methods

### Chemicals

Analytical grade chemicals were obtained from Sigma Chemical Co. (St. Louis, MO). Micronized triamcinolone acetonide was obtained from Sigma. Micronized budesonide was obtained from Sicor (Milan, Italy). Micronized fluticasone propionate was obtained from Glaxo-Wellcome (Research

Triangle Park, North Carolina). Lactose monohydrate NF extra fine (particle size 10-30 microns) was obtained from EM industries (Hawthorne, NY). Radiolabeled triamcinolone acetonide ({6,7-$^{3}$H} TA, 35.4 Ci/mmol) was purchased from DuPont NEN® Research Products (Boston, MA). All other reagents were of analytical grade.

IT Administration in Rats

Intravenous solutions were prepared by dissolving the glucocorticoids in a mixture of PEG 300 and saline (2:1 v/v) to obtain a final concentration of 200 μg/ml. Intratracheal dry powders were mixed by geometrically diluting glucocorticoid powders with lactose to obtain a concentration of 4 μg / mg lactose.

The Animal Care Committee of the University of Florida, an AAALAC approved facility, approved all animal procedures. Specific-pathogen-free male F-344 rats, weighing approximately 220 to 250 grams, were housed in a 12 hr light/dark cycle / constant temperature environment. Animals were allowed free access to water and rat chow, but were food-fasted overnight prior to each experiment.

The animals were housed in the operating room 12 hours before the experiment to get them accustomed to the new environment. The day of the experiment the rats were handled gently to produce minimum stress. Once weighed, the rats were placed in a rat holder for intraperitoneal administration of the anesthetic (fresh preparation of the combination of 1.5 ml of ketamine 10%,

1.5 ml of xylazine 2% and 0.5 ml of acepromazine 1%) at the dose of 1 ml/kg. The depth of anesthesia was checked by tail pinch or pedal withdrawal reflex.

The neck of the completely anesthetized animal was shaved and aseptically cleaned with isopropyl alcohol 70%. A one-centimeter midline vertical incision was made originating above the sternal notch. The neck muscles and glands were carefully dissected midline, until the trachea was exposed and a tracheotomy was performed between the third and fourth tracheal rings. One inch of a 14 gauge Novalon catheter sheath attached to a delivery device for intratracheal administration of dry powders (Penn-Century, Philadelphia, PA), was introduced into the trachea. A mixture of 5 $\pm$ 0.5 mg (calibrated with lactose, n=16) of extra fine monohydrate lactose and TA, BUD, or FP (0.4%, 100 $\mu$g/kg dose) was placed in the chamber of the device and instilled in the lungs with insufflation of 3 ml of air. A sham rat was included in each set of experiments that received 5 mg of the vehicle (lactose). Animals (one animal per time point) including sham rat, were decapitated at 0.5, 1, 2, 4, 6, or 12 hours after instillation. Lung, liver, kidney, spleen and brain were immediately processed for receptor binding studies. A total of six to nine independent experiments for TA, BUD, and FP, respectively, were performed for a given time point after IT administration.

IV Administration in Rats

For the intravenous (IV) injection of budesonide, animals were anesthetized as described above and the intracardial approach was used. For this approach, IV solution was injected after placement in the heart and verified

by aspiration of blood. Either 100 μl of IV solution (200 μg/ml drug) or 100μl of the vehicle (for the sham rat) was slowly injected using a tuberculin syringe with a 27-gauge needle. Animals (one animal per time point) including sham rat, were decapitated at ½, 1, 2, 4, 6, or 12 hours after instillation. Lung, liver, kidney, spleen and brain were immediately processed for receptor binding studies. A total of three to six independent experiments for TA (previously reported [160]), BUD, FP were performed for a given time point after IV administration.

*Ex Vivo* Receptor Binding Assay

An *ex vivo* receptor binding assay previously described [125] was employed with minor modifications. Briefly, immediately after decapitation, the lungs (without trachea), a lobe of the liver, kidney, spleen, and brain were resected and placed on ice. The weighed tissue was added to 10 times (for liver and spleen) and 4 times (lung, kidney, and brain) organ weight of ice-cooled incubation buffer (10 mM Tris/HCl, 10 mM sodium molybdate, 2 mM 1,4-dithiothreitol). The mixture was then homogenized in a Virtis 45 homogenizer at 40% of full speed, for three periods of 5 seconds each with a 30-second cooling period between each step. One-tenth volume of 5% activated charcoal (prepared in incubation buffer) was added to the homogenate and mixed. After 5 minutes, the suspension was centrifuged at 4°C at 50,000g for 10 min. in a Beckman centrifuge equipped with a JA-21 rotor (Beckman instruments, Palo Alto, CA) to obtain a clear supernatant. Aliquots of the supernatant (150 μl) were transferred into microcentrifuge tubes that contained 25 μl of $^{3}$H-triamcinolone acetonide in

incubation buffer (final concentration 10 nM) and 25 μl of incubation buffer or 25 μl of unlabeled TA (10 μM) to determine total and non-specific binding respectively. Aliquots of 150 μl of the resultant cytosol preparations were transferred into microcentrifuge tubes which contained 25 μl of $^{3}$H-triamcinolone acetonide in incubation buffer (10 nM final concentration) and 25 μl of incubation buffer to determine the amount of total radioactivity. After a 16-24 hour incubation period at 4°C, the unbound glucocorticoid was removed by addition of a 5% suspension of activated charcoal in buffer (200 μl). The mixture was incubated for 5 min on ice and then centrifuged at 10,000 rpm for 5 min in a micro-centrifuge (Fisher model 235A). The radioactivity (dpm) in 300 μl of supernatant was determined using a liquid scintillation counter (Beckman model LS 5000 TD, Palo Alto, CA).

All determinations were performed in triplicate and mean values for the specific binding in sham rats collected after all intratracheal or intravenous administration were used to determine 100 % free receptor level for individual data sets. Specific binding estimates found in the individual tissues differed slightly between IV (n=12, lung=1.25 nM, kidney=0.74 nM, liver=1.01 nM, and brain=0.35 nM) and IT (n=30, lung=1.01 nM, kidney=0.72 nM, liver=1.08 nM, and brain=0.40 nM) shams.

Non-Compartmental Analysis

In order to quantify the receptor binding in each tissue and degree of pulmonary targeting the area-under-the-effect-curve ($AUEC_{organ}$) up to six hours was calculated for each investigation set by the trapezoidal rule from percent free receptors vs. time profiles for both the local and systemic organs. The 12 hour time

point was not included in these calculations as the data density between 6 and 12 hours was not sufficient and for ease of comparison with previous studies [125].

Pulmonary targeting was defined as:

$$PT = AUEC_{Lung} - AUEC_{sys\ organ} \quad \text{(eq. 3.1)}$$

where $AUEC_{sys\ organ}$ represents the AUEC of liver, spleen, kidney, or brain. All data is reported as mean ± standard deviation of three or 6 independent experiments. Differences in AUEC's between lung and systemic organs were tested for significance using unpaired Student's T-test ($p<0.05$).

For comparison of the pulmonary targeting between different drugs after IT administration, the difference in pulmonary targeting (using liver and kidney as the systemic organ) was defined as

$$\text{Diff. in } PT = PT_{drug\ 1} - PT_{drug\ 2} \quad \text{(eq. 3.2)}$$

Where Drug 1 and 2 are TA, BUD, or FP. Differences in PT between drug treatments were tested for significance using unpaired Student's T-test.

The mean pulmonary effect time was calculated from $AUEC_{\infty}$ and $AUMEC_{\infty}$ according to equation 3.3

$$MET = AUMEC_{\infty} / AUEC_{\infty} \quad \text{(eq. 3.3)}$$

where $AUMEC_{0\rightarrow\infty}$ is the area under the first moment curve, and $AUEC_{0\rightarrow\infty}$ is the area under the curve. The area under the curve ($AUEC_{0\rightarrow\infty}$) was calculated by the trapezoidal rule from the E versus time curve ($AUEC_{0\rightarrow12}$) and extrapolation to infinity ($AUEC_{12\rightarrow\infty}$) calculated by adding the ratio of the last $E_{12}$ measured and the first-order rate constant of the terminal phase ($k_e$). The area under the first moment curve ($AUMEC_{0\rightarrow\infty}$) was calculated from the E * t versus time curve ($AUMEC_{0\rightarrow12}$) and extrapolation to infinity ($AUMEC_{12\rightarrow\infty}$) calculated by adding the ratio of the last measured $E_{12}$ * t and the squared of the rate constant of elimination ($E_{12} * t / k_e + E_{12} / k_e^2$).

## Results

### Receptor-Binding of TA after IT Administration in Rats

The resulting receptor occupancy versus time profiles after intratracheal administration of triamcinolone acetonide dry powders are shown in Figure 3.1 and AUEC's reported in Table 3.1. There was a significant difference in receptor occupancies between lung versus kidney ($p<0.01$) and lung versus brain ($p<0.01$), while lung versus liver ($p>0.1$) and lung versus spleen ($p>0.4$) receptor occupancies resulted in close superimposition. The pulmonary MET was 4.4 hours.

### Receptor-Binding of TA after IV Administration in Rats

The resulting receptor occupancy versus time profile after intravenously administered triamcinolone acetonide solutions is shown in Figure 3.2 and AUEC's reported in Table 3.1 as previously reported [160]. There was

no significant difference in receptor occupancies between lung versus liver ($p>0.20$), resulting in close superimposition. The pulmonary MET was 2.8 hours.

Receptor-Binding of BUD after IT Administration in Rats

The resulting receptor occupancy versus time profiles after intratracheally administered budesonide dry powder are shown in Figure 3.3 and AUEC's reported in Table 3.1. There was a significant difference in receptor occupancies between lung versus brain ($p<0.01$), while no targeting was observed for lung versus liver ($p>0.1$), lung versus kidney ($p>0.2$), and lung versus spleen ($p>0.3$). The pulmonary MET was 3.6 hours.

Receptor-Binding of BUD after IV Administration in Rats

The resulting receptor occupancy versus time profiles after intravenously administered budesonide solutions are shown in Figure 3.3 and AUEC's reported in Table 3.1. There was a significant difference in receptor occupancies between lung versus brain ($p<0.01$), while no targeting was observed for lung versus liver ($p>0.4$), lung versus kidney ($p>0.3$), and lung versus spleen ($p>0.3$). The pulmonary MET was 3.1 hours.

Receptor-Binding of FP after IT Administration in Rats

The resulting receptor occupancy versus time profiles after intratracheally administered fluticasone propionate dry powders are shown in Figure 3.5 and AUEC's reported in Table 3.1. There was a significant difference in receptor occupancies between lung versus liver ($p<0.01$), lung versus kidney ($p<0.01$), lung versus spleen ($p<0.01$), and lung versus brain ($p<0.01$). The pulmonary MET was 4.1 hours.

Receptor-Binding of FP after IV Administration in Rats

The resulting receptor occupancy versus time profiles after intravenous administered fluticasone propionate solutions are shown in Figure 3.6 and AUEC's reported in Table 3.1. There was a significant difference in receptor occupancies between lung versus liver ($p<0.02$) and lung versus brain ($p<0.01$), while no targeting was observed for lung versus kidney ($p>0.2$) and lung versus spleen ($p>0.3$). The pulmonary MET was 5.5 hours.

Comparison of Pulmonary Targeting between Drug Formulations

Differences in pulmonary targeting between TA vs. BUD, TA vs. FP, BUD vs. FP (using liver and kidney for comparison) are reported in Table 3.2. Statistical significance was measured using unpaired Student's t-test between individual AUEC's. There was no significant difference between TA vs. BUD using kidney or liver as the systemic organ ($p>0.4$ and $p>0.05$, respectively). For TA vs. FP there was a significant difference using liver as the systemic organ ($p<0.01$), while there was no difference using the kidney as the systemic organ ($p>0.3$). For BUD vs. FP both liver and kidney showed a significant difference ($p<0.01$ for both).

## Discussion

These experiments assessed the pulmonary targeting of triamcinolone acetonide (TA), budesonide (BUD), and fluticasone propionate (FP) after intratracheal (IT) and intravenous (IV) administration *in vivo* in rats. As stated in Chapter 2, intravenous administration was compared with intratracheal

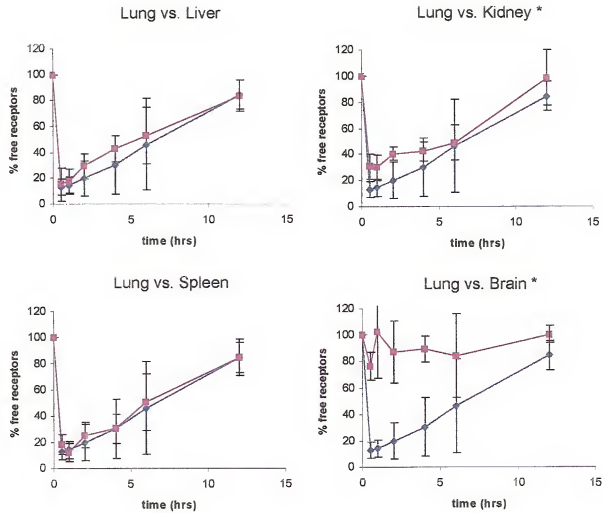


Figure 3.1: Receptor occupancy time profiles after intratracheal administration of triamcinolone acetonide-dry powder (100 μg/kg): A) lung ◆ versus liver ■ (n=9**), B) lung ◆ versus spleen ■ (n=9**), C) lung ◆ versus kidney ■ (n=9**), and D) lung ◆ versus brain ■, (n=3).

* denotes $p < 0.05$ between AUEC's (0-6 hrs).
** n=6 previously reported from [151].

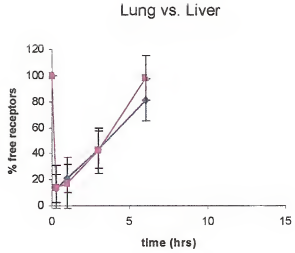


Figure 3.2: Receptor occupancy time profile after intravenous administration of triamcinolone acetonide solution (100 μg/kg): A) lung ◆ versus liver ■ (n=6**).

** previously reported from [151].

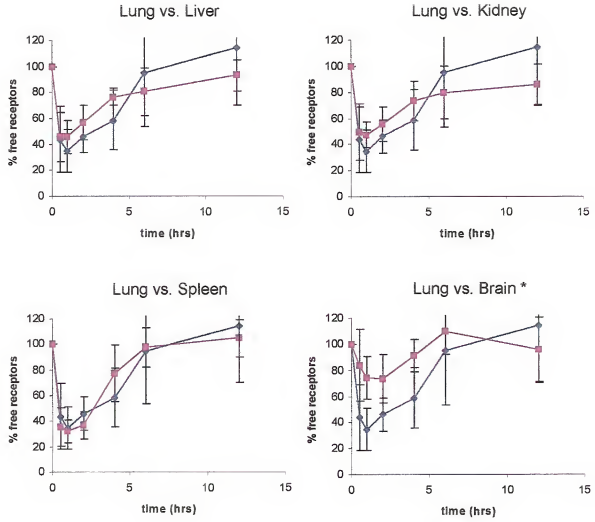


Figure 3.3: Receptor occupancy time profiles after intratracheal administration of budesonide-dry powder (100 µg/kg): A) lung ◆ versus liver ■ (n=6), B) lung ◆ versus spleen ■ (n=6), C) lung ◆ versus kidney ■ (n=6), and D) lung ◆ versus brain ■, (n=6).

* denotes $p < 0.05$ between AUEC's (0-6 hrs).

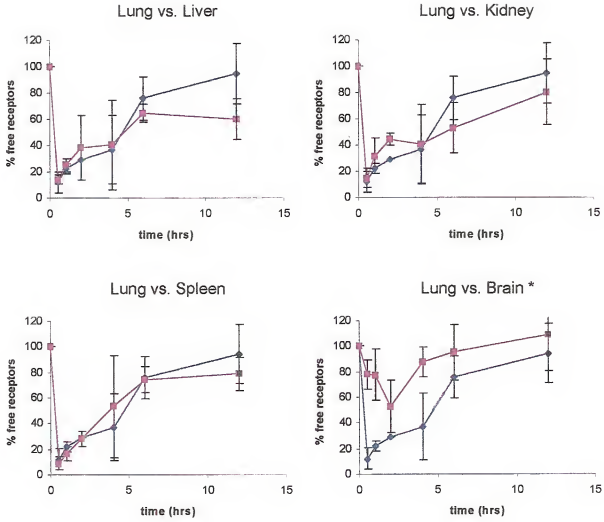


Figure 3.4: Receptor occupancy time profiles after intravenous administration of budesonide solution (100 μg/kg): A) lung ◆ versus liver ■ (n=3), B) lung ◆ versus spleen ■ (n=3), C) lung ◆ versus kidney ■ (n=3), and D) lung ◆ versus brain ■, (n=3).

* denotes $p < 0.05$ between AUEC's (0-6 hrs).

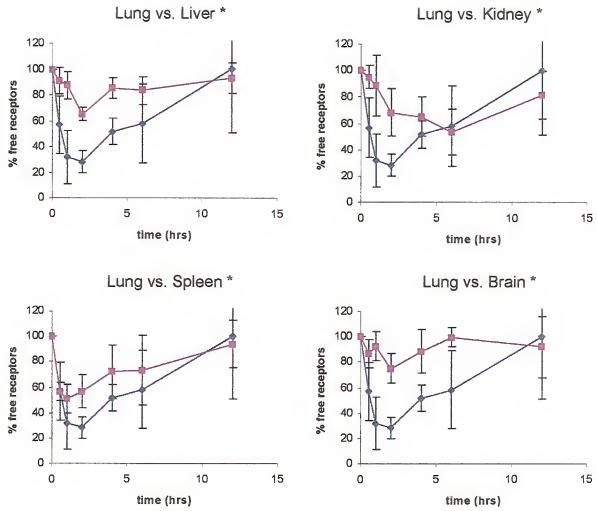


Figure 3.5: Receptor occupancy time profiles after intratracheal administration of fluticasone propionate-dry powder (100 μg/kg): A) lung ◆ versus liver ■ (n=9**), B) lung ◆ versus spleen ■ (n=9**), C) lung ◆ versus kidney ■ (n=9**), and D) lung ◆ versus brain ■, (n=6).

* denotes $p < 0.05$ between AUEC's (0-6 hrs).
** n=3 previously reported from [151].

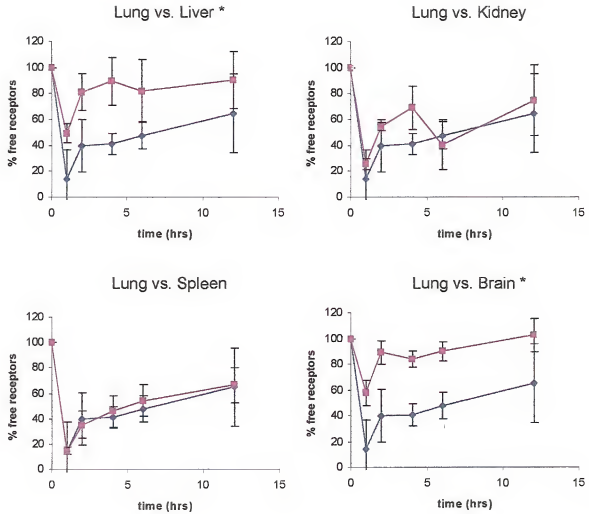


Figure 3.6: Receptor occupancy time profiles after intravenous administration of fluticasone propionate solution (100 μg/kg): A) lung ◆ versus liver ■ (n=6), B) lung ◆ versus spleen ■ (n=6), C) lung ◆ versus kidney ■ (n=6), and D) lung ◆ versus brain ■, (n=3).

* denotes $p < 0.05$ between AUEC's (0-6 hrs).

Table 3.1: Mean area-under-the-effect-curve (AUEC) and pulmonary targeting (PT) values for each glucocorticoid.

| | **TA IT** (n=9)* | **TA IV** (n=6)** | **BUD IT** (n=6) | **BUD IV** (n=3) | **FP IT** (n=9)*** | **FP IV** (n=3) |
|---|---|---|---|---|---|---|
| | **AUEC (%*hr)** | | | | | |
| $AUEC_{lung}$ | 419 ± 76 | 303 ± 81 | 245 ± 102 | 350 ± 55 | 317 ± 90 | 396 ± 110 |
| $AUEC_{liver}$ | 379 ± 48 | 322 ± 77 | 197 ± 62 | 337 ± 104 | 109 ± 40 | 211 ± 127 |
| $AUEC_{kidney}$ | 322 ± 41 | | 204 ± 57 | 334 ± 65 | 194 ± 79 | 349 ± 108 |
| $AUEC_{spleen}$ | 415 ± 43 | | 223 ± 64 | 327 ± 65 | 229 ± 110 | 381 ± 62 |
| $AUEC_{brain}$ | 68 ± 40 | | 72 ± 61 | 124 ± 64 | 76 ± 58 | 108 ± 20 |
| | **Pulmonary Targeting (%*hr)** | | | | | |
| $AUEC_{lung}$ - $AUEC_{liver}$ | 52 ± 47 | -19 ± 6 | 49 ± 64 | 13 ± 52 | **208 ± 77** | **185 ± 74** |
| $AUEC_{lung}$ - $AUEC_{kidney}$ | **110 ± 90** | | 41 ± 63 | 17 ± 18 | **123 ± 79** | 48 ± 74 |
| $AUEC_{lung}$ - $AUEC_{spleen}$ | 17 ± 58 | | 22 ± 64 | 24 ± 18 | **87 ± 55** | 16 ± 64 |
| $AUEC_{lung}$ - $AUEC_{brain}$ | **290 ± 137** | | **173 ± 46** | **226 ± 26** | **216 ± 110** | **231 ± 120** |
| | **Pulmonary Mean Effect Time (hr)** | | | | | |
| $MET_{lung}$ | 4.4 | 2.8 | 3.6 | 3.1 | 4.1 | 5.5 |

* n=6 previously reported from [151], n=3 for brain.
** previously reported from [160].
** n=3 previously reported from [151], n=6 for brain.
**Boldface** denotes $p < 0.05$ between AUEC's (0-6 hrs).

Table 3.2: Differences in PT and calculated P-values (unpaired T-test) comparing pulmonary targeting of TA vs. BUD, TA vs. FP, BUD vs. FP after IT administration (using the liver and kidney for systemic organs only).

| | **Difference in PT** |
|---|---|
| TA vs. BUD - $PT_{liver}$ | 3.9 |
| TA vs. BUD - $PT_{kidney}$ | 69 |
| TA vs. FP - $PT_{liver}$ | **156** |
| TA vs. FP - $PT_{kidney}$ | 13 |
| BUD vs. FP - $PT_{liver}$ | **160** |
| BUD vs. FP - $PT_{kidney}$ | **82** |

**Boldface** denotes $p < 0.05$ between AUEC's (0-6 hrs).

administration to calculate differences in pulmonary targeting and MET due to absorption in the lungs.

Several *in vitro* and *in vivo* studies have shown differences in the topical and systemic potency [161], receptor affinity [162, 163], and pharmacokinetic properties [11, 74, 78] of inhaled glucocorticoids. In addition, pharmacokinetic / pharmacodynamic (PK/PD) models have been developed to assess the extent of glucocorticoid systemic effects such as lymphocyte and cortisol suppression [117]. These studies, however, give no direct indication of the extent of pulmonary selectivity, as it is determined by both the extents of local, as well as systemic effects. Furthermore, pulmonary targeting is difficult to evaluate in humans because good surrogate markers for pulmonary effects are not available for pharmacological studies [8]. In this study we used the *ex vivo* receptor-binding assay previously described to assess pulmonary selectivity of three commercially available inhaled glucocorticoids in different organs.

Our group previously assessed pulmonary targeting of TA after intravenous administration by monitoring the receptor occupancy in lung and liver only. We have shown that the IV administration of TA resulted in liver receptor occupancies that were not significantly different from those in lung, indicating no targeting. This is in agreement with the expected lack of targeting upon IV administration.

In the present study we have considered not only the liver as a marker for the extent of systemic exposure, but other tissues such as the kidney, spleen, and brain. This was primarily done because of concerns that the high

intrinsic hepatic clearance of fluticasone propionate may affect the receptor binding results. The overall level of pulmonary targeting was determined by comparing the lung AUEC (% free receptors vs. time) to the systemic organ AUEC (% free receptors vs. time) up to six hours as previously described [125]. Although differences in the AUEC's up to six hours are representative of the level of pulmonary targeting, for the same drug differences in AUEC's between administration routes (IV vs. IT) can be observed most likely due to differences in absorption.

Upon intravenous administration of BUD we found that lung, liver, kidney, and spleen had similar receptor binding profiles, but that the brain had significantly less receptor binding, similar to IT administration of TA. Although the brain has been shown to have a high concentration of glucocorticoid receptors, cumulative brain receptor binding was less pronounced than those observed in the other systemic organs, indicating that the distribution of drug to this organ is affected by other factors [164]. These factors might include a lack of efficient distribution across the blood-brain barrier or the effect of a p-glycoprotein efflux pump [97, 98]. The similar binding profiles for lung, liver, kidney, and spleen are in agreement with the expected distribution pattern of glucocorticoids to highly perfused organs.

The intravenous administration of FP resulted in similar receptor binding profiles for lung, kidney, and spleen. Again, the brain receptor occupancies were significantly different from those in the lung. But contrary to BUD and TA, the hepatic receptor occupancies for FP were significantly less

than the pulmonary receptor occupancies as well. This difference was not due to metabolism of FP during *ex vivo* incubation, which was confirmed by the FP-receptor complex demonstrating high stability under normal assay conditions (unpublished results). This significant difference in lung and liver receptor occupancies after IV administration was not expected, since the free drug concentrations and receptor occupancies should be similar throughout the body (assuming no tissue sequestration). But if the high intrinsic hepatic clearance of FP is considered, the lower liver receptor occupancy observed may be understandable. Because FP is highly metabolized in the liver (which is also indicated by its oral bioavailability of lower than 1%), at any given time point both free drug concentrations and liver receptor occupancies should be lower than those in the other organs. These findings suggest that the monitoring the receptor binding in the liver and lung alone may not be an appropriate method to assess the extent of systemic effects of drugs with high intrinsic hepatic clearance such as fluticasone propionate.

The intratracheal administration of TA, BUD, and, to a certain degree, FP resulted in close superimposition of lung and spleen receptor occupancies. It is well known that glucocorticoids induce the redistribution of several blood cells to different lymphatic organs including spleen [165]. Recently it has also been suggested that the glucocorticoid receptor density in immune organs, such as the spleen, is higher than other organs (higher $B_{max}$), which may amplify the receptor occupancy after glucocorticoid administration compared to other systemic organs [166]. This would indicate that the spleen might not be an

adequate systemic organ to assess the degree of glucocorticoid spill over into the systemic circulation.

The intratracheal administration of BUD dry powder (100 μg/kg) resulted in liver, kidney, and spleen receptor occupancies that were not significantly lower than the lung receptor occupancy. Similar findings have been reported using the Sephadex-induced lung edema model, where budesonide displayed similar local vs. systemic effects [167]. The pulmonary MET after IV administration was 3.1 hours compared to after IT administration of 3.6 hours, showing a relatively similar difference in mean effect times (0.5 hour) compared with the mean residence times (0.2 hour) as seen in Chapter 2. This data suggests that fast dissolution and absorption of budesonide dry powders results in limited pulmonary targeting.

Intratracheal administration of TA dry powder (100 μg/kg) resulted in similar receptor occupancies for spleen and lung, while receptor occupancies for kidney and brain were significantly lower than those for lung. Although these results suggest that there is a higher pulmonary targeting for TA than BUD, the kidney receptor occupancies for previously reported data sets showed high non-specific binding [151]. If the last three data sets performed were considered separately (with modifications made to decrease non-specific binding), pulmonary targeting was not statistically significant between the lung and kidney receptor occupancies. The difference in pulmonary mean effect times (1.6 hours) showed a greater difference than the mean residence times (0.2 hour)

found in Chapter 2, but may also be due to differences in experimental techniques in previously assessing TA after IV administration [160].

The intratracheal administration of FP dry powder resulted in receptor occupancies that were significantly lower for liver, kidney, spleen, and brain than those for lung. The lower hepatic receptor occupancies is likely due to the combined effects of high intrinsic clearance (similar to IV results) and slower absorption of pulmonary-delivered FP, suggesting that the kidney may be a more applicable organ to assess FP pulmonary selectivity. The pulmonary mean effect time after IV administration was 5.5 hours compared to the MET after IT administration of 4.1 hours, which is comparable to the calculated mean residence time in plasma after IT administration of 5.6 hours (Chapter 2). The high pulmonary mean effect time after IV administration is mainly due to the sustained receptor occupancy out to 12 hours, which should be confirmed through further experiments.

Overall, fluticasone propionate showed the highest level of pulmonary targeting in multiple organs. As seen in Chapter 3, the dissolution rates *in vitro* and the absorption rates *in vivo* were similar for TA and BUD, while FP was significantly slower. Fluticasone propionate showed superior pulmonary targeting versus triamcinolone acetonide when comparing lung receptor occupancies to those in liver and budesonide when comparing lung receptor occupancies to those in liver and kidney. Considering the differences in receptor binding of fluticasone propionate to triamcinolone acetonide and budesonide, we can observe that drug formulations with slower dissolution and absorption rates

result in an increase in pulmonary targeting. To further analyze this relationship of increasing pulmonary targeting by controlling the dissolution rate, a sustained release formulation of budesonide will be evaluated in Chapter 4.

## Conclusions

- Budesonide did not display statistically significant pulmonary targeting when comparing lung receptor occupancies to those in liver and kidney.
- Triamcinolone acetonide did not display statistically significant pulmonary targeting when comparing lung receptor occupancies to those in liver.
- Fluticasone propionate showed superior pulmonary targeting when comparing lung receptor occupancies to those in liver and kidney.
- Fluticasone propionate, which had the lowest dissolution and absorption rate as seen in Chapter 3, showed a high level of pulmonary targeting.
- Considering the differences in receptor binding of fluticasone propionate to triamcinolone acetonide and budesonide, we can observe that glucocorticoid powders with slower dissolution rates have higher pulmonary targeting.

# CHAPTER 4
# CHARACTERIZATION, *IN VITRO* DISSOLUTION, AND *IN VIVO* PLASMA CONCENTRATIONS AND PULMONARY TARGETING IN RATS OF A NOVEL SUSTAINED-RELEASE FORMULATION OF MICROENCAPSULATED BUDESONIDE

## Introduction

Currently, dry-powder inhalers (DPI) are used to deliver various drugs to the lungs for localized or systemic delivery. Although current formulations and delivery systems are adequate for pulmonary drug therapy, they are limited by potential problems with pulmonary deposition characteristics as well as the residence time of the drug after inhalation ([14], also seen in Chapter 2). Previously, liposomes were used by our group as a model sustained release system with a substantial improvement in pulmonary targeting in rats [125]. Liposomes and microspheres have been investigated as sustained release delivery systems for the lung [34, 69], but because of complicated manufacturing and wet processing, a novel dry-coating technique previously developed for engineered particulates using pulsed laser deposition (PLD) is proposed [146]. It is proposed that modification of the release rate of the drug from dry powders by applying a biodegradable polymer coating would greatly enhance the pulmonary residence time, and thus improve pulmonary targeting.

Over the past few years, the pulsed laser deposition (PLD) technique has emerged as one of the simplest and most versatile methods for the deposition of thin films of a wide variety of materials [168]. The stoichiometric removal of the constituent species from the target during ablation (i.e. monomer and nanoclusters of polymer) from a polymer target, as well as the relatively small number of control parameters, are the two major advantages of PLD over some of the other physical vapor-deposition techniques. No studies have currently been performed using biodegradable polymers for coating materials by PLD, so comparison of the molecular structure of the deposited films to original material was performed to ensure that the polymer structure remained intact after deposition.

Overall the objective of this section was to use PLD to ablate a target of a biodegradable polymer, poly(lactic-co-glycolic) acid (PLGA 50:50), to coat budesonide (BUD) micronized drug particles for 10 (BUD10) and 25 (BUD25) minute runs. Characterization of films deposited on silicon wafers or glass slides was performed using SEM, FTIR, and NMR to characterize polymer structure and morphology. Then BUD10 and BUD25 coated powders were tested *in vitro* to assess differences in the dissolution rates. Then BUD25 coated drug formulation was administered intratracheally *in vivo* in rats to monitor plasma concentration and improvement in pulmonary targeting. Comparison of the plasma concentrations after IT administration of the coated powders with uncoated BUD powders and IV administration of BUD solution in Chapter 2, as well as with FP after IT administration, will be performed to compare absorption

rates. Finally, the pulmonary targeting of coated BUD25 powders after IT administration was compared with the pulmonary targeting of uncoated BUD and FP powders after IT administration and BUD solution after IV administration in Chapter 3.

## Hypothesis

Sustained release formulations of budesonide with a slower dissolution rate *in vitro* will have a slower absorption rate and improved pulmonary targeting *in vivo*.

## Materials and Methods

### Chemicals

Analytical grade chemicals were obtained from Sigma Chemical Co. (St. Louis, MO.). Micronized budesonide was obtained from Sicor (Milan, Italy). Poly(lactic-co-glycolic acid) 50:50 DL high intrinsic viscosity (Lot# 3097-204) was purchased from Medisorb Medical Technologies, Inc., Cinncinnati, Ohio. Lactose monohydrate NF extra fine (particle size 10-30 microns) was obtained from EM industries Hawthorne, NY. Radiolabeled triamcinolone acetonide ({6,7-$^{3}$H} TA, 35.4 Ci/mmol) was purchased from DuPont NEN® Research Products (Boston, MA). All other reagents were of analytical grade.

Pulsed Laser Deposition (PLD) Setup

We have used the PLD procedure to deposit films of biodegradable polymers, namely poly(lactic-co-glycolic acid) (PLGA), onto glucocorticoid drug particles in the micrometer range. The PLGA target was heat pressed in a 0.15 cm x 3.5 cm x 3.5 cm mold using a carver press at 120° C. The coating procedure consists of the polymer target (PLGA) and fluidized bed of micronized drug powder (500 mg batch) contained within a vacuum chamber. The 248 nm laser pulse at 150 mJ and 5 hertz enters the vacuum chamber through a quartz window and ablates the polymer target. The surface of the target material is rapidly heated and expands from the surface into the vacuum atmosphere to form a plume. The plume of low-molecular weight polymer chains then adheres to the drug particle as agglomerates. Preliminary coatings on silicon wafers were performed to examine plume uniformity and coating thickness. Coating runs were performed using 500 mg of free drug powders and coated for 10 minutes (BUD10) and 25 minutes (BUD25).

SEM Analysis

Polymer coatings on silicon wafers and micronized drug powders were analyzed using a Joel model 6400 EDS scanning electron microscope (SEM) to obtain information on the size, shape, and surface morphology. Micrographs of powder samples were prepared by applying a thin layer of carbon paint onto a graphite sample mount and spreading approximately one milligram on top. Sample mounts then underwent a carbon evaporation process prior to

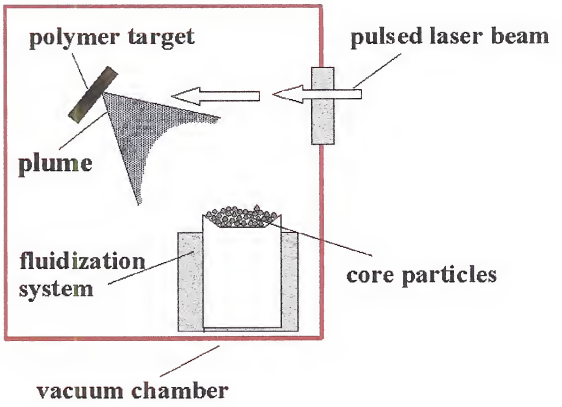


Figure 5.1: Pulsed laser deposition (PLD) setup for coating drug particles with polymer coating.

characterization. Characterization was performed at 1-2 kEV in vacuum. Magnification of representative micrographs was x 5,500.

NMR Analysis

For characterization of polymer structure, proton nuclear magnetic resonance ($^1$H-NMR) analysis was performed as previously reported for PLGA [169] using a Varian NMR (Model VXR, 300 MHz). Samples for analysis on silicon wafers after 2-minute runs were dissolved in deuterated chloroform with 1% TMS (Sigma, Inc.) and approximately 1 ml transferred to NMR glass tubes for analysis. Standard parameters were acquisition time 4.0 sec, relaxation delay 1.0 sec, 16 scan repetitions, and pulse width 3,600 hz were used (standard $^1$H-NMR program).

FTIR Analysis

Fourier-transform infrared spectroscopy (FTIR) was also used to characterize the polymer structure as previously reported [170] using a Nicolet Magna 760 FTIR with OMNIC 3.0 software. Diffuse reflectance of films on glass slides was monitored using the DRIFTS module and subtracting spectra for uncoated glass slide. For PLGA analysis 10 mg of polymer was dissolved in 2 ml of methylene chloride and cast on a glass slide and the solvent evaporated. For deposited PLGA, a glass slide was placed under the PLGA target and deposited for 5 minutes.

*In Vitro* Dissolution

*In vitro* dissolution of free drug (BUD), 10 minute coated drug (BUD10), and 25 minute coated drug (BUD25) formulations (500 mg of 2% drug

in lactose) were tested using a USP dissolution bath (VanKel Technology Group, Cary, NC) in 900 ml of pH 7.4 phosphate-buffered saline (50 mM, 0.5% SDS) at 37° C. After drug was added one-milliliter samples were removed and filtered through a 0.2 μm syringe filter at 0, 0.5, 1, 1.5, 2, 2.5, 5, 10, 15, 30, 45, 60, 75, 90, 105, 120, and 600 minutes and analyzed using HPLC. Steady state was reached at 600 minutes (observed from release profiles) and replaced as 100% dissolved (for free powder) or released (for coated powders).

Glucocorticoid concentrations in solution were analyzed using an HPLC setup consisting of a Perkin Elmer series 3B pump with a flow rate of 1.0 ml/min and a Zorbax C-18 (150 x 4.6 mm) column connected to a Perkin Elmer ISS 100 autoinjector. The detector was a Milton Roy SM-4000 attached to a Hewlett Packard HP-3394A integrator. The eluent was monitored at 254 nm. The mobile phase consisted of a mixture of 50%:50% v/v acetonitrile : 0.03% triflouroacetic acid buffer for BUD. Samples were injected after standards (5 standards of 1, 5, 10, 50, and 100 μg/ml) for each data set. Slopes from the calibration curve from standards were used to calculate the sample concentration for each data set ($r^2$>0.99).

Half-life of dissolution ($t_{50\%}$) for the free powder was calculated by curve fitting using SCIENTIST program and using the monoexponential formula:

$$\text{Cumulative \% Dissolved} = 100 - [\, A * \exp^{-\alpha t} \,] \qquad \text{(eq. 4.1)}$$

to obtain the dissolution rate constant ($\alpha$) for the free powder. The half-lives of release ($t_{50\%}$) for the coated powders were calculated by the biexponential formula:

$$\text{Cumulative \% Released} = 100-[(A*\exp^{-\alpha t})+(B*\exp^{-\beta t}] \quad \text{(eq. 4.2)}$$

to obtain the dissolution rate constants ($\alpha$ and $\beta$). Half-lives of dissolution ($t_{50\%}$) were calculated as $0.693/\alpha$ for free powders and $0.693/\beta$ for coated powders.

Differences in dissolution between drug formulations were tested for significance using the FDA scale-up and postapproval changes (SUPAC) similarity test ($f_2$):

$$f_2 = 50 \text{ x LOG } \{[1+1/n \Sigma(R_t-T_t)^2]^{-0.5} \text{ x } 100\} \quad \text{(eq. 4.3)}$$

where n=17 time points (0, 0.5, 1, 1.5, 2, 2.5, 5, 10, 15, 30, 45, 60, 75, 90,105,120, and 600 minutes), $R_t$ = the reference % drug dissolved at time t, and $T_t$. = the test % drug dissolved at time t. An $f_2$ value between 50 and 100 suggests the two dissolution profiles are similar and an $f_2$ value less than 100 indicates a lack of similarity [153].

IT Administration in Rats

The Animal Care Committee of the University of Florida, an AAALAC approved facility, approved all animal procedures. Specific-pathogen-free male F-344 rats, weighing approximately 220 to 250 grams, were housed in

a 12 hr light/dark cycle / constant temperature environment. Animals were allowed free access to water and rat chow, but were food-fasted overnight prior to each experiment.

The animals were housed in the operating room 12 hours before the experiment to get them accustomed to the new environment. The day of the experiment the rats were handled gently to produce minimum stress. Once weighed, the rats were placed in a rat holder for intraperitoneal administration of the anesthetic (fresh preparation of the combination of 1.5 ml of ketamine 10%, 1.5 ml of xylazine 2% and 0.5 ml of acepromazine 1%) at the dose of 1 ml/kg. The depth of anesthesia was checked by tail pinch or pedal withdrawal reflex.

The neck of the completely anesthetized animal was shaved and aseptically cleaned with isopropyl alcohol 70%. A one-centimeter midline vertical incision was made originating above the sternal notch. The neck muscles and glands were carefully dissected midline, until the trachea was exposed and a tracheotomy was performed between the third and fourth tracheal rings. One inch of a 14 gauge Novalon catheter sheath attached to a delivery device for intratracheal administration of dry powders (Penn-Century, Philadelphia, PA), was introduced into the trachea. A mixture of 5 ± 0.5 mg (calibrated with lactose, n=16, see Chapter 2) of extra fine monohydrate lactose and coated budesonide (BUD25) (0.4%, 100 μg/kg dose) was placed in the chamber of the device and instilled in the lungs with insufflation of 3 ml of air. A sham rat was included in each set of experiments that received 5 mg of the vehicle (lactose). Animals (one animal per time point) including sham rat, were decapitated at ½, 1, 2, 4, 6,

or 12 hours after instillation. Plasma was snap frozen and stored at -70°C until processing. A total of four independent experiments for BUD25 was performed for a given time point after IT administration.

Solid Phase Extraction of Plasma Samples

Frozen plasma samples were thawed at room temperature. A volume of 200 μl plasma was added to 1.8 ml of 10% ethanol with 10 ng/ml final concentration of internal standard (TA for BUD analysis). Recovery from the extraction technique was measured by spiking blank plasma with 10 ng/ml final concentration of BUD standard for each sample set. Solid phase extraction (SPE) of compounds was performed as previously described with modifications [154][Li, 1997 #8]. Briefly, samples with 10% ethanol were refrigerated for 15 minutes to precipitate proteins and centrifuged at 4000 rpm. Supernatants were then extracted using ethanol-activated 6 ml endcapped C-18 cartridges (Supelco). The analytes were eluted with 2 x 1 ml of 60% ethyl acetate in heptane. The residue was evaporated under vacuum and reconstituted in 100 μl of methanol-water (80:20, v/v) mobile phase. A total sample volume of 80 μl was injected into the HPLC-APCI/MS/MS system.

LC/MS/MS of Extracted Plasma Samples

The analysis of BUD was performed as described previously for FP with modifications [155]. A Micromass Quattro-LC-Z (Beverly, MA) triple quadrupole mass spectrometer equipped with an atmospheric pressure chemical ionization (APCI) ion source was used for analysis. The APCI probe temperature was set to 500° C and corona and cone voltages were set at optimum conditions

after tuning. The MS/MS signals were optimized by injecting a 1 μg/ml standard in methanol at a flow-rate of 100 μl/min using a Kd-Scientific® infusion pump. At low collision energy, mass analysis was collected through the second quadrople for 428.0>428.0 for BUD. Argon was used as the collision gas at $1.5 \times 10^{-3}$ mBar. The mass spectrometer was linked to a Perkin Elmer ISS-200 autosampler via contact closure and the operation was controlled by computer software, Masslynx 3.1. The mobile phase was a mixture of methanol-water (80:20, v/v) delivered at a flow-rate of 1.2 ml/min by a LDC/ Milton Roy CM4000 multiple solvent delivery system. Chromatographic separations were achieved using a Waters 5-μm ODS2 (4.6 x 50 mm i.d.) column (Milford, MA) preceded by a Whatman 5-μm ODS C–18 guard column cartridge (Clifton, NJ). Data analysis was performed using Masslynx software. Samples were injected with calibration curves (4 standards of 1, 10, 20, and 100 ng/ml) for each data set. Slopes from concentration vs. peak area profiles were used for each data set ($r^2$>0.99) and plasma concentrations calculated by multiplying by (Area / Slope) * 2 / Recovery. Recovery from SPE was calculated as 64.1 ± 3.2% for BUD (n=12).

*Ex Vivo* Receptor Binding Assay

An *ex vivo* receptor binding assay previously described [125] was employed with minor modifications. Briefly, immediately after decapitation, the lungs (without trachea), a lobe of the liver, kidney, spleen, and brain were resected and placed on ice. The weighed tissue was added to 10 times (for liver and spleen) and 4 times (lung, kidney, and brain) organ weight of ice-cooled incubation buffer (10 mM Tris/HCl, 10 mM sodium molybdate, 2 mM 1,4-

dithiothreitol). The mixture was then homogenized in a Virtis 45 homogenizer at 40% of full speed, for three periods of 5 seconds each with a 30-second cooling period between each step. One-tenth volume of 5% activated charcoal (prepared in incubation buffer) was added to the homogenate and mixed. After 5 minutes, the suspension was centrifuged at 4°C at 50,000g for 10 min. in a Beckman centrifuge equipped with a JA-21 rotor (Beckman instruments, Palo Alto, CA) to obtain a clear supernatant. Aliquots of the supernatant (150 μl) were transferred into microcentrifuge tubes that contained 25 μl of $^{3}$H-triamcinolone acetonide in incubation buffer (final concentration 10 nM) and 25 μl of incubation buffer or 25 μl of unlabeled TA (10 μM) to determine total and non-specific binding respectively. Aliquots of 150 μl of the resultant cytosol preparations were transferred into microcentrifuge tubes which contained 25 μl of $^{3}$H-triamcinolone acetonide in incubation buffer (10 nM final concentration) and 25 μl of incubation buffer to determine the amount of total radioactivity. After a 16-24 hour incubation period at 4°C, the unbound glucocorticoid was removed by addition of a 5% suspension of activated charcoal in buffer (200 μl). The mixture was incubated for 5 min on ice and then centrifuged at 10,000 rpm for 5 min in a micro-centrifuge (Fisher model 235A). The radioactivity (dpm) in 300 μl of supernatant was determined using a liquid scintillation counter (Beckman model LS 5000 TD, Palo Alto, CA). All determinations were performed in triplicate and mean values for the specific binding in sham rats collected during the last couple of years were used to determine 100 % free receptor level for individual data sets.

Non-Compartmental Pharmacokinetic Analysis

The non-compartmental analysis for plasma concentrations over time was performed using standard techniques [156]. The time to peak $t_{max}$ (at $C_{max}$) and peak $C_{max}$ was determined as the highest plasma concentration from the average plasma concentration vs. time profile.

Mean residence time (MRT) for plasma data was calculated from the relationship:

$$MRT_{0\rightarrow\infty} = AUMC_{0\rightarrow\infty} / AUC_{0\rightarrow\infty} \qquad \text{(eq. 4.4)}$$

where $AUMC_{0\rightarrow\infty}$ is the area under the first moment curve, and $AUC_{0\rightarrow\infty}$ is the area under the curve. The area under the curve ($AUC_{0\rightarrow\infty}$) was calculated by the trapezoidal rule from the C versus time curve ($AUC_{0\rightarrow12}$) and extrapolation to infinity ($AUC_{12\rightarrow\infty}$) calculated by adding the ratio of the last measured concentration ($C_{12}$) and the first-order rate constant of the terminal phase ($k_e$, exponential regression from 4 to 12 hours, $r^2>0.97$) . The area under the first moment curve ($AUMC_{0\rightarrow\infty}$) was calculated from the C * t versus time curve ($AUMC_{0\rightarrow12}$) and extrapolation to infinity ($AUMC_{12\rightarrow\infty}$) calculated by adding the ratio of the last measured $C_{12}$ * t and the squared of the rate constant of elimination ($C_{TAL}*t/k_e + C_{TAL}/k_e^2$).

Differences in AUC's between IV and IT administration were tested for significance using unpaired Student's T-test. The total body clearance (Cl)

was calculated as dose divided by $AUC_{0\rightarrow\infty}$ divided by the pulmonary bioavailability (Dose/AUC*F).

Mean absorption time for BUD was calculated from the relationship:

$$MAT = MRT_{IT} - MRT_{IV} \quad \text{(eq. 4.5)}$$

Where BUD25 was compared to BUD IV and compared to the pharmacokinetic data collected for BUD IT vs. BUD IV in Chapter 2.

In order to quantify the receptor binding in each tissue and degree of pulmonary targeting, the cumulative change from baseline ($AUEC_{organ}$) up to six hours was calculated for each investigation set by the trapezoidal rule from percent free receptors vs. time profiles for both the local and systemic organs. The 12 hour time point was not included in these calculations as the data density between 6 and 12 hours was not sufficient and for ease of comparison with previous studies [125].

Pulmonary targeting was defined as:

$$PT = AUEC_{Lung} - AUEC_{sys\ organ} \quad \text{(eq. 4.6)}$$

where $AUECsys_{organ}$ represents the AUEC of liver, spleen, kidney, or brain. All data is reported as mean ± standard deviation of three or 6 independent experiments. Differences in AUEC's between lung and systemic organs were tested for significance using unpaired Student's T-test.

For comparison of the pulmonary targeting in the liver or kidney between drug regimens, the difference in pulmonary targeting was defined as

$$\text{Diff. in PT} = PT_{\text{drug 1}} - PT_{\text{drug 2}} \qquad \text{(eq. 4.7)}$$

Where Drug 1 and 2 are BUD, BUD25, or FP. Differences in PT between drug treatments were tested for significance using unpaired Student's T-test.

The mean pulmonary effect time was calculated from $AUEC_{\infty}$ and $AUMEC_{\infty}$ according to equation 4.3

$$MET = AUEC_{\infty} / AUMEC_{\infty} \qquad \text{(eq. 4.8)}$$

where $AUMEC_{0\rightarrow\infty}$ is the area under the first moment effect curve, and $AUEC_{0\rightarrow\infty}$ is the area under the effect curve. The area-under-the-effect-curve ($AUEC_{0\rightarrow\infty}$) was calculated by the trapezoidal rule from the E versus time curve ($AUEC_{0\rightarrow12}$) and extrapolation to infinity ($AUEC_{12\rightarrow\infty}$) calculated by adding the ratio of the last $E_{12}$ measured and the first-order rate constant of the terminal phase ($k_e$). The area under the first moment effect curve ($AUMEC_{0\rightarrow\infty}$) was calculated from the E * t versus time curve ($AUMEC_{0\rightarrow12}$) and extrapolation to infinity ($AUMEC_{12\rightarrow\infty}$) calculated by adding the ratio of the last measured $E_{12}$ * t and the squared of the rate constant of elimination ($E_{12} * t / k_e + E_{12} / k_e^2$).

## Results

### SEM Analysis

SEM photomicrographs of polymer coatings on silicon wafers and micronized dry powder are depicted in Figures 4.2 and 4.3, respectively. For polymer coatings on silicon wafers (Figure 4.2) average droplet size after one second was approximately 100 nm or less, with more continuous films after 2 minutes (edge of surface shown). Comparison of uncoated vs. coated particles were not quantitative (Figure 4.3), but there appeared to be no significant increase in particle size (1 to 3 microns).

### NMR Analysis

$^1$H-NMR profiles of PLGA and coated PLGA onto silicon wafers are depicted in Figure 4.4. Overlapping doublets at 1.6 ppm have been previously described for the protons on the methyl groups in the D,L-lactic acid repeat units [169]. The multiplets at 5.2 and 4.8 ppm have been shown to correspond to the lactic acid CH and the glycolic acid $CH_2$, respectively [169]. The dense regions of peaks in the multiplets have been described to be due to the complexity of the monomer peaks in the copolymer backbone [169]. Additional background peaks at 1.2, 1.8, and 3.7 could not be identified, but spectra from characteristic peaks at 1.6, 4.8 and 5.2 ppm from PLGA and deposited PLGA appeared similar.

### FTIR analysis

FTIR profiles of original PLGA and PLGA deposited onto a glass slide are depicted in Figure 4.5. Characteristic absorptions peaks seen in both

A

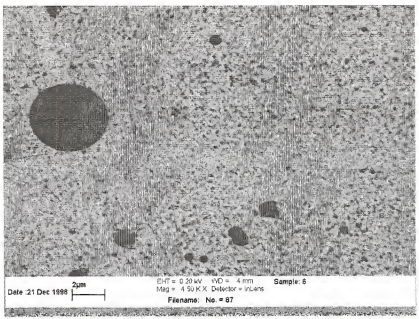


B

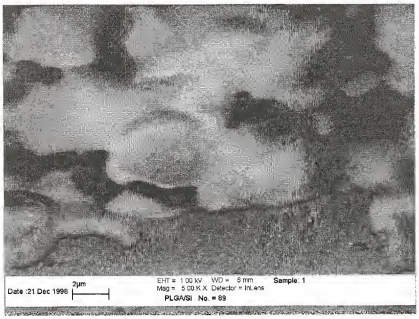


Figure 4.2: SEM micrographs of PLGA films onto silicon wafers after: A) 1 second and B) 2 minutes. Magnification 5,000 times. Droplet size ~100 nm.

A


B


Figure 4.3: SEM micrographs of: A) micronized BUD powder, and B) micronized coated BUD25 powder. Resolution 5,500 times magnification.

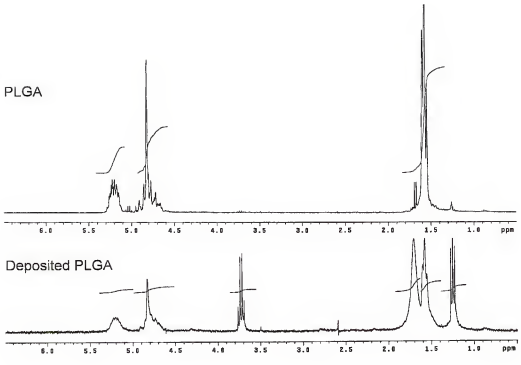


Figure 4.4: NMR of original PLGA and PLGA deposited onto a silicon wafer. The deposited PLGA sample retains the characteristic 1.6, 4.8, and 5.2 ppm peaks of original PLGA.

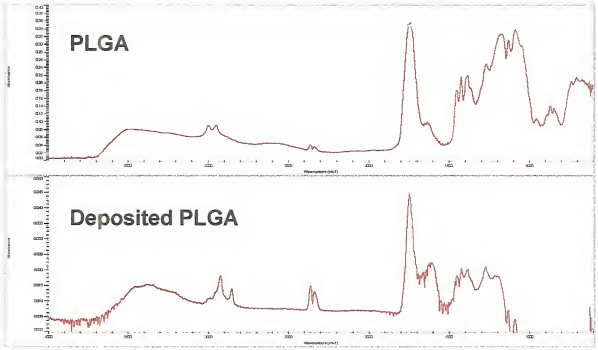


Figure 4.5: FTIR of original PLGA and PLGA deposited onto a glass slide.

profiles are a carbonyl peak at 1,760 $cm^{-1}$, methyl peak (from lactide) at 2,850 $cm^{-1}$, and carboxylate peak at 1650 $cm^{-1}$. A triple ester peak is present in both profiles around 1400 $cm^{-1}$, corresponding to monomeric units within the polymeric chain of lactide-latide (L-L) at 1456 $cm^{-1}$, glycolide-glycolide (G-G) at 1425 $cm^{-1}$, and lactide-glycolide at (L-G) at 1398 $cm^{-1}$. Spectra of deposited PLGA retain similar characteristic peaks to original PLGA suggesting deposited polymer films were intact PLGA.

*In Vitro* Dissolution

The cumulative dissolution profiles for BUD free powder and BUD10 and BUD25 coated powders are depicted in Figure 4.6. The fitted monoexponential curve for BUD free powder showed some divergance from 5 to 10 minutes, but the resulting fits showed good correlation ($r^2$>0.99) with a half-life of release ($t_{50\%}$) of 1.2 ± 0.1 minutes (n=3). Dissolution of coated powders followed the biexponential equation with an initial burst of free drug (30-40%) and half-life of release ($t_{50\%}$) of coated particles of 29 ± 0.8 minutes for BUD10 ($r^2$=0.99) 10-minute coating and 60 ± 1.6 minutes for BUD25 ($r^2$=0.99) 25 minute coating. The dissolution half-life for BUD25 was significantly slower than uncoated BUD ($f_2$=24) and BUD10 ($f_2$=42), and BUD10 was significantly slower than uncoated BUD ($f_2$=34).

Pharmacokinetics of Coated Budesonide (BUD25) in Rats

The average budesonide plasma concentration after IT administration of BUD25 (n=4) is shown in Figure 4.7 (together with BUD IV and BUD IT from Chapter 2 shown for comparison). The pharmacokinetic

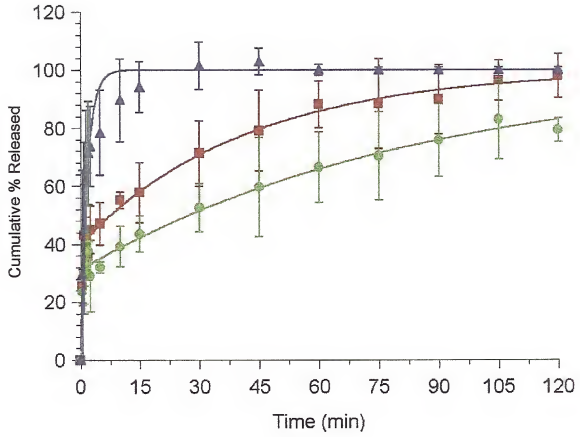


Figure 4.6: Dissolution of uncoated budesonide vs. coated budesonide in pH 7.4 PBS (50 mM, 0.5 % SDS) at 37°C (n=3). Profiles are shown for uncoated budesonide powder (BUD) ▲, and coated powders after 10 minute (BUD10) ■ and 25 minute (BUD25) • runs.

parameters resulting from the analysis of plasma data for BUD25 are listed in Tables 4.1 (together with BUD IV, BUD IT, and FP IT from Chapter 2). The maximum budesonide plasma concentration from BUD25 after IT administration was 128.4 ng/ml at 1.0 hour. The terminal slope ($k_e$) was 0.19 $hr^{-1}$ ($r^2$=0.99) and the $AUC_{0\rightarrow\infty}$ was 222 ± 62.3 ng/ml*hr after IT administration of coated powders. The mean residence time (MRT) was calculated as 3.2 hours after BUD25 IT administration, with a resulting mean absorption time (MAT) of 0.8 hour.

Table 4.1 Pharmacokinetic parameters for BUD25.

| | BUD IV | BUD IT | BUD25 IT | FP IT |
|---|---|---|---|---|
| $C_{max}$ (ng/ml) | 29.3 | 48.1 | 128.4 | 15.2 |
| $t_{max}$ (hr) | 0.5 | 0.5 | 1.0 | 1.0 |
| $k_e$ ($hr^{-1}$) | 0.26 | 0.33 | 0.19 | 0.22 |
| AUC (ng/ml*hr) | 60.6 ± 26.9 | 85.3 ± 41.2 | 222 ± 62.3 | 92.0 ± 54.5 |
| MRT (hr) | 2.4 | 2.7 | 3.2 | 5.6 |
| MAT (hr) | | 0.3 | 0.8 | |

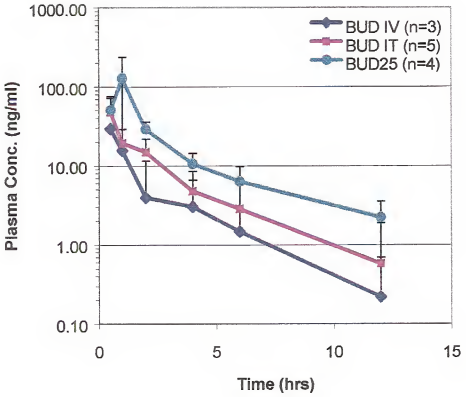


Figure 4.7 Average plasma concentrations (mean ± SD) after IV administration of BUD IV(n=3) and IT administration of BUD free powders (n=5) and BUD25 coated powders (n=4).

Receptor-Binding of Coated Budesonide (BUD25) in Rats

The resulting receptor occupancy versus time profiles after intratracheally administered budesonide coated dry powders (BUD25) are shown in Figure 4.8 and pulmonary targeting reported in Table 4.2. There was a significant difference in receptor occupancies between lung versus liver ($p<0.03$), lung versus kidney ($p<0.01$), and lung versus brain ($p<0.01$), while no targeting was observed for lung versus spleen ($p>0.1$). Pulmonary targeting was most pronounced for lung versus brain, followed by lung versus kidney, lung versus liver, and lung versus spleen. The pulmonary MET was calculated to be 5.5 hours.

Comparison of Pulmonary Targeting between Drug Formulations

Differences in pulmonary targeting between BUD free powders, BUD25 coated powders, and FP free powders (using liver and kidney for comparison) are reported in Table 4.3. Statistical significance was measured using unpaired Student's t-test between individual AUEC's. For BUD vs. BUD25 there was a significant difference using kidney as the systemic organ ($p<0.01$), while there was no difference using the liver as the systemic organ ($p>0.1$). For BUD vs. FP, as discussed in Chapter 3, both liver and kidney showed a significant difference ($p<0.01$ for both). For BUD25 vs. FP, there was no significant difference using kidney or liver as the systemic organ ($p>0.05$ for both).

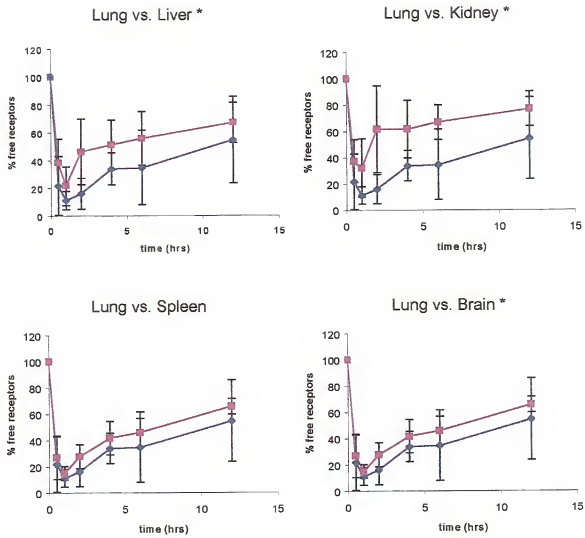


Figure. 4.8: Receptor occupancy time profiles after intratracheal administration of BUD25 coated powders (100 µg/kg): A) lung ◆ versus liver ■ (n=4), B) lung ◆ versus spleen ■ (n=4), C) lung ◆ versus kidney ■ (n=4), and D) lung ◆ versus brain ■, (n=4).

* denotes $p < 0.05$ between AUEC's (0-6 hrs).

Table 4.2: Mean area-under-the-effect-curve (AUEC) and pulmonary targeting (PT) values for each glucocortioid.

| | **BUD IV** (n=3) | **BUD IT** (n=6) | **BUD25 IT** (n=4) | **FP IT** (n=9)** |
|---|---|---|---|---|
| | **AUEC (%*hr)** | | | |
| $AUEC_{lung}$ | 350 ± 55 | 245 ± 102 | 429 ± 60 | 317 ± 90 |
| $AUEC_{liver}$ | 337 ± 104 | 197 ± 62 | 312 ± 75 | 109 ± 40 |
| $AUEC_{kidney}$ | 334 ± 65 | 204 ± 57 | 250 ± 90 | 194 ± 79 |
| $AUEC_{spleen}$ | 327 ± 65 | 223 ± 64 | 380 ± 39 | 229 ± 110 |
| $AUEC_{brain}$ | 124 ± 64 | 72 ± 61 | 136 ± 42 | 76 ± 58 |
| | **Pulmonary Targeting (%*hr)** | | | |
| $AUEC_{lung}$ – $AUEC_{liver}$ | 13 ± 52 | 49 ± 64 | **117 ± 102** | **208 ± 77** |
| $AUEC_{lung}$ – $AUEC_{kidney}$ | 17 ± 18 | 41 ± 63 | **180 ± 50** | **123 ± 79** |
| $AUEC_{lung}$ – $AUEC_{spleen}$ | 24 ± 18 | 22 ± 64 | 50 ± 78 | **87 ± 55** |
| $AUEC_{lung}$ – $AUEC_{brain}$ | **226 ± 26** | **173 ± 46** | **293 ± 88** | **216 ± 110** |
| | **Pulmonary Mean Effect Time (hr)** | | | |
| $MET_{ung}$ | 3.1 | 3.6 | 5.5 | 4.1 |

** denotes n=6 for brain
**Boldface** denotes $p < 0.05$ between AUEC's (0-6 hrs).

Table 4.3: Differences in PT and calculated P-values (unpaired T-test) comparing pulmonary targeting of BUD vs. BUD25, BUD vs. FP, BUD25 vs. FP using the liver and kidney.

| | Difference in PT (P-value) |
|---|---|
| BUD vs. BUD25 - $PT_{liver}$ | 68 |
| BUD vs. BUD25 - $PT_{kidney}$ | **139** |
| BUD vs. FP - $PT_{liver}$ | **160** |
| BUD vs. FP - $PT_{kidney}$ | **82** |
| BUD25 vs. FP - $PT_{liver}$ | 92 |
| BUD25 vs. FP - $PT_{kidney}$ | -56 |

**Boldface** denotes $p < 0.05$ between differences in PT's (0-6 hrs).

## Discussion

In the present study we investigated the use of a novel coating technique for controlled release of budesonide *in vitro* and *in vivo* in rats. Verification of deposited polymer on silicon wafers using NMR and FTIR was used to characterize molecular structure. Then, the use of a coated particle formulation of budesonide (BUD25) with slower dissolution characteristics *in vitro* was delivered *in vivo* in rats to observe differences in absorption and pulmonary targeting. Free powders of budesonide (BUD) and fluticasone propionate (FP) were used for comparison. As discussed in Chapters 3 and 4, BUD with a faster absorption rate *in vivo* showed little pulmonary targeting and FP with a slower absorption rate showed greater pulmonary targeting.

Although the comparison of particle size and morphology using SEM was more or less qualitative and not quantitative, SEM photomicrographs of the polymeric coatings after deposition show the relatively nanometer thick level of coatings formed using the PLD technique. SEM photomicrographs of polymer deposited onto silicon wafers at different run times suggested that 100 nanometer size or less droplets are deposited and form continuous coatings after several minutes. SEM photomicrographs comparing uncoated particles to coated particles showed no observable difference in particle size after coating, but this is difficult to quantitate with standard techniques at the nanometer level. Further analysis should be performed to accurately quantitate the coating structure and thickness, but HPLC analysis of dissolved coated powders in

solution compared to pure powder showed polymer mass was less than 0.1% weight.

Analysis of the polymer samples using FTIR and NMR verified that the deposited polymer retained its molecular structure after deposition. Analysis using FTIR was successful in confirming that the general composition peaks of the polymer backbone did not change dramatically after deposition. Characterization using NMR also showed similar characteristic peaks between PLGA deposited on silicon wafers and original PLGA. Both techniques were not quantitative, though, because the sensitivity and the scans are dependant on the amount of material used, and as stated above only a small amount of polymer is deposited using this technique.

Dissolution analysis *in vitro* of BUD10 (10 minute coating) and BUD25 (25 minute coating) showed biphasic dissolution rates with $T_{50\%}$ of 29 and 60 minutes, respectively. There appears to be an early release of uncoated drug in the first 5 minutes, and then a slow release of drug from coated particles over 1-2 hours. This release may be beneficial to obtain therapeutic levels immediately, while the coated portion released over 1-2 hours maintains concentrations close to therapeutic levels longer while reducing systemic spillover.

The peak plasma concentration of BUD25 after intratracheal administration was at 1.0 hour (vs. 0.5 hours for free powders). While the AUC appears to be higher than for the free BUD powders, verification of powder formulations showed an approximately two-fold increase in the dose

administered to rats. The MAT was calculated to be 0.8 hour vs. 0.3 hour for the free powder, interestingly similar to the *in vitro* dissolution half-life of 1.0 hour. Although this change in the *in vitro* dissolution and *in vivo* absorption rate was an improvement, further studies should be performed with coatings of longer dissolution rate to further evaluate the relationship of dissolution rate on absorption rate and pulmonary targeting.

The receptor-binding profiles for BUD25 showed an improvement in pulmonary targeting over BUD free powders in the lung vs. liver and lung vs. kidney, and a higher pulmonary targeting than FP when comparing the receptor binding profiles in the lung vs. kidney. In addition, the pulmonary MET increased almost two hours to 5.5 hours compared to 3.6 hours after the free powder. Previously shown in Chapter 2, FP was shown to have the slowest *in vitro* dissolution rate and with a later $t_{max}$ and MRT *in vivo* suggested a longer absorption rate. Also in Chapter 3 FP was shown to have superior pulmonary targeting when compared to TA and BUD free powders. Now, by considering the improvement in pulmonary targeting by only changing the dissolution rate of budesonide, this strongly suggests that the increase in pulmonary targeting of BUD25 coated powders is obtained by controlling the release rate of budesonide into the lung.

Currently, there is much interest in controlling release of biotechnology and gene therapy agents in the lungs [69]. Other techniques including low-density microspheres [69], spray-coated microparticles [171], conventional microspheres [172], and liposomes [85, 125] have been researched

but currently none have reached FDA approval. Reports of increases in the pulmonary half-lives up to 18 hours of locally active agents in liposome formulations have been shown [173, 174]. In particular, the plasma concentration profiles and pulmonary targeting of liposome encapsulated triamcinolone acetonide phosphate showed an increase in the mean absorption time from liposomal release (5.6 hours) and resulted in a statistically significant increase in pulmonary targeting [125]. Although the PLGA coated budesonide dry powders presented in this chapter only resulted in an increase in the MAT of 0.8 hour when compared to uncoated budesonide, a statistically significant increase in pulmonary targeting was also observed. This would indicate that small changes in the release rate of pulmonary drug formulations enhances the local vs. systemic effects observed, but more *in vivo* studies should be performed to evaluate this relationship.

The use of this microencapsulation technique using PLD suggests that because of the relative flexibility in applying varying amounts of polymer onto the drug particles, the industrial applicability should be excellent. The process also has several advantages over current techniques including: (1) it is a fast process with modification times on the order of minutes, (2) a variety of materials can be used for producing the coatings on the particulate materials, thus it is possible to produce films from materials with proven biocompatibility, (3) it is a dry, solvent-less technique that can be conducted under a sterile environment, which is an important consideration in the drug industry, (4) particle agglomeration/adhesion can theoretically be minimized by applying coatings that

affect the bonding nature and electrostatic charge on the surface, (5) from a toxicological point of view, applying nano-thick polymer coatings is likely to show advantages over traditional polymeric microspheres by significantly reducing the inhaled polymer load (<1% by weight polymer).

## Conclusions

- Coatings of PLGA were analyzed by SEM, NMR, and FTIR, and proved that thin coatings of polymer of varying thicknesses could be applied by controlling the run-time.
- Dissolution of coated budesonide BUD25 particles *in vitro* were biphasic, with a slower dissolution rate of 59.5 minutes after a 25 minute run.
- Plasma concentrations after IT administration of BUD25 showed a slower absorption rate than free powders with a MAT of 0.8 hours.
- Receptor-binding profiles of BUD25 showed that coated powders gained a statistically significant increase in pulmonary targeting compared to uncoated BUD powders and FP powders, suggesting a substantial improvement in therapeutic efficacy of slow-releasing coated particles.

# CHAPTER 5
# CONCLUSIONS

The overall objective of this thesis was to compare the dissolution rates *in vitro*, and pharmacokinetics and pulmonary targeting *in vivo* of three currently available inhaled glucocorticoid dry powders (triamcinolone acetonide, budesonide, and fluticasone propionate) and one sustained release formulation (microencapsulated budesonide). First, dissolution of fluticasone propionate was shown to be slower than triamcinolone acetonide and budesonide *in vitro*. *In vivo* experiments investigating plasma concentrations after intratracheal and intravenous administration using LC/MS/MS showed comparable fast absorption times for budesonide and triamcinolone acetonide and a later peak plasma concentration and longer MRT for fluticasone propionate suggesting slower absorption. Also, the trend in calculated clearances of the three glucocorticoids studied showed a similar trend in rats with published human studies (TA>FP>BUD). Pulmonary targeting was measured using an *ex vivo* receptor-binding assay to measure the level of bound drug to the glucocorticoid receptor in multiple organs at different times. Using this method, fluticasone propionate showed the highest level of pulmonary targeting followed by triamcinolone acetonide and budesonide. Then, to evaluate the use of a new sustained-release formulation, microencapsulated budesonide dry powder was investigated

as an improved sustained release model. SEM analysis showed that polymer coatings did not substantially increase particle size, while *in vitro* dissolution half-life increased ten-fold. The pharmacokinetic profile *in vivo* showed slower absorption for coated budesonide than free dry-powder formulations. Finally, *ex vivo* receptor binding of coated budesonide showed a statistically significant increase in pulmonary targeting when compared to free powders of budesonide and fluticasone propionate. This method of extending the release-rate of the encapsulated material using polymeric-coated particles has promising industrial applications, and further emphasizes the relationship between increasing pulmonary residence time to improve pulmonary targeting.

## REFERENCES


1. Nicklas, R.A., National and international guidelines for the diagnosis and treatment of asthma. *Curr Opin Pulm Med*, 1997. **3**(1): 51-5.

2. Brogden, R.N., Heel, R.C., Speight, T.M., and Avery, G.S., Beclomethasone dipropionate. A reappraisal of its pharmacodynamic properties and therapeutic efficacy after a decade of use in asthma and rhinitis. *Drugs*, 1984. **28**(2): 99-126.

3. Brogden, R.N. and McTavish, D., Budesonide. An updated review of its pharmacological properties, and therapeutic efficacy in asthma and rhinitis. *Drugs*, 1992. **44**(3): 375-407.

4. Holliday, S.M., Faulds, D., and Sorkin, E.M., Inhaled fluticasone propionate. A review of its pharmacodynamic and pharmacokinetic properties, and therapeutic use in asthma. *Drugs*, 1994. **47**(2): 318-31.

5. Pakes, G.E., Brogden, R.N., Heel, R.D., Speight, T.M., and Avery, G.S., Flunisolide: a review of its pharmacological properties and therapeutic efficacy in rhinitis. *Drugs*, 1980. **19**(6): 397-411.

6. Spencer, C.M. and McTavish, D., Budesonide. A review of its pharmacological properties and therapeutic efficacy in inflammatory bowel disease. *Drugs*, 1995. **50**(5): 854-72.

7. Lipworth, B.J., Clinical pharmacology of corticosteroids in bronchial asthma. *Pharmacol Ther*, 1993. **58**(2): 173-209.

8. Kelly, H.W., Establishing a therapeutic index for the inhaled corticosteroids: part I. Pharmacokinetic/pharmacodynamic comparison of the inhaled corticosteroids. *J Allergy Clin Immunol*, 1998. **102**(4 Pt 2): S36-51.

9. Kamada, A.K., Szefler, S.J., Martin, R.J., Lazarus, S.C., and Lemanske, R.F., Issues in the use of inhaled glucocorticoids. *Am J Respir Crit Care Med*, 1996. **153**: 1739-1748.

10. Derendorf, H., Hochhaus, G., Meibohm, B., Moellmann, H., and Barth, J., Pharmacokinetics and pharmacodynamics of inhaled corticosteroids. *J Allergy Clin Immunol*, 1998. **101**(4 Pt 2): S440-6.

11. Edsbaecker, S. and Szefler, S.J., *Glucocorticoid pharmacokinetics - principles and clinical applications*, in *Inhaled glucocorticoids in asthma*, R.P. Schleimer, W.W. Busse, and P.M. O'Byrne, Editors. 1997, Marcel Dekker, New York: 381-445.

12. Johnson, M., Pharmacodynamics and pharmacokinetics of inhaled glucocorticoids. *J Allergy Clin Imm*, 1996. **97**: 169-76.

13. Pavord, I. and Knox, A., Pharmacokinetic optimisation of inhaled steroid therapy in asthma. *Clin Pharmacokinet*, 1993. **25**(2): 126-35.

14. Hochhaus, G., Moellmann, H., Derendorf, H., and Gonzalez-Rothi, R., Pharmacokinetic / pharmacodynamic aspects of aerosol therapy using glucocorticoids as a model. *J Clin Pharmacol*, 1997. **37**: 881-892.

15. Rohdewald, P., Moellmann, H., and Hochhaus, G., Affinities of glucocorticoids for glucocorticoid receptors in the human lung. *Agents and Action*, 1985. **17**: 290-291.

16. Mueller, M. and Renkawitz, R., The glucocorticoid receptor. *Biochemica et Biophsica Acta*, 1991. **1088**: 171-182.

17. Evans, R.M., The steroid and thyroid hormone receptor superfamily. *Science*, 1988. **240**: 889-895.

18. McConnell, W. and Howarth, P., The airway anti-inflammatory effects of fluticasone propionate. *Rev Contemp Pharmacother*, 1998. **9**: 523-533.

19. Bamberger, C.M., Bamberger, A.M., de Castro, M., and Chrousos, G.P., Glucocorticoid receptor beta, a potential endogenous inhibitor of glucocorticoid action in humans. *J Clin Invest*, 1995. **95**(6): 2435-41.

20. Munck, A., Mendel, D.B., Smith, L.I., and Orti, E., Glucocorticoid Receptors and Actions. *American Reviews of Respiratory Diseases*, 1990. **141**: S2-S10.

21. Jusko, W.J., Corticosteroid pharmacodynamics: Models for a broad array of receptor-mediated pharmacodynamic effects. *J Clin Pharmacol*, 1990. **30**: 303-310.

22. Didonato, J.A., Molecular mechanisms of immunosuppresion and anti-anflammatory activities by glucocorticoids. *Am J Resp Crit Care Med*, 1996. **154**: S11-S15.

23. Schleimer, R.P., Effects of glucocorticosteroids on inflammatory cells relevant to their therapeutic applications in asthma. *Am Rev Respir Dis*, 1990. **141**(2 Pt 2): S59-69.

24. Reed, C.E., New therapeutic Approaches in Asthma. *J Allergy Clin Immunol*, 1986. **77**(4): 537-543.

25. Barnes, P.J., New concepts in the pathogenesis of bronchial hyperresponsiveness and asthma. *J Allergy Clin Immunol*, 1989. **83**(6): 1013-26.

26. Barnes, P.J., Our changing understanding of asthma. *Resp Med*, 1989. **83**: S17-S23.

27. Silberstein, D.S. and David, J.R., The regulation of human eosinophil function by cytokines. *Immunol Today*, 1987. **8**: 380-5.

28. Barnes, P.J., Molecular mechanisms of antiasthma therapy. *Ann Med*, 1995. **27**(5): 531-5.

29. Schwiebert, L.A., Beck, L.A., Stellato, C., Bickel, C.A., Bochner, B.S., and Schleimer, R.P., Glucocorticosteroid inhibition of cytokine production: relevance to antiallergic actions. *J Allergy Clin Immunol*, 1996. **97**(1 Pt 2): 143-52.

30. Pratt, W.B., Glucocorticoid receptor structure and the initial events in signal transduction. *Mol End Ster Horm Action*, 1990: 119-132.

31. Barnes, P.J., Asthma. New therapeutic approaches. *Br Med Bull*, 1992. **48**(1): 231-47.

32. Barnes, P.J., Inhaled glucocorticoids: new developments relevant to updating of the asthma management guidelines. *Respir Med*, 1996. **90**(7): 379-84.

33. Laitinen, L.A., Laitinen, A., Heino, M., and Haahtela, T., Eosinophilic airway inflammation during exacerbation of asthma and its treatment with inhaled corticosteroid. *Am Rev Respir Dis*, 1991. **143**(2): 423-7.

34. Zeng, X., Martin, G., and Marriott, C., The Controlled Delivery of Drugs to the Lungs. *Int J Pharm*, 1995. **124**: 149-164.

35. Paterson, J.W., Woolcock, A.J., and Shenfield, G.M., Bronchodilator drugs. *Am Rev Respir Dis*, 1979. **120**(5): 1149-88.

36. Newman, S., Steed, K., Hooper, G., Kallen, A., and Borgstroem, L., Comparison of gamma scintigraphy and a pharmacokinetic technique for assessing pulmonary deposition of terbutaline sulphate delivered by pressurized metered dose inhaler. *Pharm Res*, 1995. **12**(2): 231-6.

37. Pauwels, R., Newman, S., and Borgstroem, L., Airway deposition and airway effects of antiasthma drugs delivered from metered-dose inhalers. *Eur Respir J*, 1997. **10**(9): 2127-38.

38. Borgstroem, L. and Nilsson, M., A method for determiniation of the absolute pulmonary bioavailability of inhaled drugs: Terbutaline. *Pharm Res*, 1990. **7**(10): 1068-1070.

39. Gonda, I., A semi-empirical model of aerosol deposition in the human respiratory tract for mouth inhalation. *J Pharm Pharmacol*, 1981. **33**(11): 692-6.

40. Adjei, A. and Garren, J., Pulmonary delivery of peptide drugs: effect of particle size on bioavailability of leuprolide acetate in healthy male volunteers. *Pharm Res*, 1990. **7**(6): 565-9.

41. Newman, S.P., Moren, F., Pavia, D., Little, F., and Clarke, S.W., Deposition of pressurized suspension aerosols inhaled through extension devices. *Am Rev Respir Dis*, 1981. **124**(3): 317-20.

42. Newman, S.P., Aerosol deposition considerations in inhalation therapy. *Chest*, 1985. **88**(2 Suppl): 152S-160S.

43. Newman, S.P., Weisz, A.W., Talaee, N., and Clarke, S.W., Improvement of drug delivery with a breath actuated pressurised aerosol for patients with poor inhaler technique. *Thorax*, 1991. **46**(10): 712-6.

44. Ganderton, D., General factors influencing drug delivery to the lung. *Respir Med*, 1997. **91 Suppl A**: 13-6.

45. Agertoft, L. and Pedersen, S., Importance of the inhalation device on the effect of budesonide. *Arch Dis Child*, 1993. **69**(1): 130-3.

46. Agertoft, L. and Pedersen, S., Influence of spacer device on drug delivery to young children with asthma. *Arch Dis Child*, 1994. **71**(3): 217-9.

47. Ahrens, R., Lux, C., Bahl, T., and Han, S.H., Choosing the metered-dose inhaler spacer or holding chamber that matches the patient's need: evidence that the specific drug being delivered is an important consideration. *J Allergy Clin Immunol*, 1995. **96**(2): 288-94.

48. Barry, P.W. and C, O.C., The effect of delay, multiple actuations and spacer static charge on the in vitro delivery of budesonide from the Nebuhaler. *Br J Clin Pharmacol*, 1995. **40**(1): 76-8.

49. Selroos, O. and Halme, M., Effect of a volumatic spacer and mouth rinsing on systemic absorption of inhaled corticosteroids from a metered dose inhaler and dry powder inhaler. *Thorax*, 1991. **46**(12): 891-4.

50. Farr, S.J., Rowe, A.M., Rubsamen, R., and Taylor, G., Aerosol deposition in the human lung following administration from a microprocessor controlled pressurised metered dose inhaler. *Thorax*, 1995. **50**(6): 639-44.

51. Ward, M.E., Woodhouse, A., Mather, L.E., Farr, S.J., Okikawa, J.K., Lloyd, P., Schuster, J.A., and Rubsamen, R.M., Morphine pharmacokinetics after pulmonary administration from a novel aerosol delivery system. *Clin Pharmacol Ther*, 1997. **62**(6): 596-609.

52. Newman, S., Steed, K., Reader, S., Hooper, G., and Zierenberg, B., Efficient delivery to the lungs of flunisolide aerosol from a new portable hand-held multidose nebulizer. *J Pharm Sci*, 1997. **85 960-4**: 960-964.

53. Newman, S.P., Brown, J., Steed, K.P., Reader, S.J., and Kladders, H., Lung deposition of fenoterol and flunisolide delivered using a novel device for inhaled medicines: comparison of RESPIMAT with conventional metered-dose inhalers with and without spacer devices. *Chest*, 1998. **113**(4): 957-63.

54. Srichana, T., Martin, G.P., and Marriott, C., Dry powder inhalers: the influence of device resistance and powder formulation on drug and lactose deposition in vitro. *Eur J Pharm Sci*, 1998. **7**(1): 73-80.

55. Thorsson, L., Edsbaecker, S., and Conradson, T.B., Lung deposition of budesonide from Turbuhaler is twice that from a pressurized metered-dose inhaler P-MDI. *Eur Respir J*, 1994. **7**(10): 1839-44.

56. Hill, L.S. and Slater, A.L., A comparison of the performance of two modern multidose dry powder asthma inhalers. *Respir Med*, 1998. **92**(1): 105-10.

57. Lipworth, B.J. and Clark, D.J., Comparative lung delivery of salbutamol given via Turbuhaler and Diskus dry powder inhaler devices. *Eur J Clin Pharmacol*, 1997. **53**(1): 47-9.

58. Devadason, S.G., Everard, M.L., MacEarlan, C., Roller, C., Summers, Q.A., Swift, P., Borgstroem, L., and Le Souef, P.N., Lung deposition from the Turbuhaler in children with cystic fibrosis. *Eur Respir J*, 1997. **10**(9): 2023-8.

59. Hardy, J.G., Newman, S.P., and Knoch, M., Lung deposition from four nebulizers. *Respir Med*, 1993. **87**(6): 461-5.

60. Harvey, C.J., O'Doherty, M.J., Page, C.J., Thomas, S.H., Nunan, T.O., and Treacher, D.F., Comparison of jet and ultrasonic nebulizer pulmonary aerosol deposition during mechanical ventilation. *Eur Respir J*, 1997. **10**(4): 905-9.

61. Pedersen, S., Inhalers and nebulizers: which to choose and why. *Respir Med*, 1996. **90**(2): 69-77.

62. Demoly, P., Jaffuel, D., Sahla, H., Bousquet, J., Michel, F.B., and Godard, P., The use of home nebulizers in adult asthma. *Respir Med*, 1998. **92**(4): 624-7.

63. Leflein, J., Brown, E., Hill, M., Kelly, H.W., Loffert, D.T., Nelson, H.S., and Szefler, S.J., Delivery of glucocorticoids by jet nebulization: aerosol characteristics and output. *J Allergy Clin Immunol*, 1995. **95**(5 Pt 1): 944-9.

64. Hochhaus, G., Suarez, S., Gonzales-Rothi, R.J., and Schreier, H., *Pulmonary targeting of inhaled glucocorticoids: How is it influenced by formulation?*, in *Respiratory Drug Delivery VI*, R. Dalby, P. Byron, and S.J. Farr, Editors. 1998, Interpharm Press, Interpharm Press: 45-52.

65. Eccles, R. and Mygind, N., Physiology of the upper airways in allergic disease. *Clin Rev Allergy*, 1985. **3**(4): 501-16.

66. Brain, J.D. and Valberg, P.A., Deposition of aerosol in the respiratory tract. *Am Rev Respir Dis*, 1979. **120**(6): 1325-73.

67. Meisner, D., *Liposomes as a pulmonary drug delivery system.* Pharmaceutical particulate carriers, ed. A. Rolland. 1993, New York: Marcel, Dekker. 31-63.

68. Schlesinger, R.B., Effects of inhaled acids on respiratory tract defense mechanisms. *Environ Health Perspect*, 1985. **63**: 25-38.

69. Edwards, D.A., et al., Large porous particles for pulmonary drug delivery. *Science*, 1997. **276**(5320): 1868-71.

70. Byron, P.R., Prediction of drug residence times in regions of the human respiratory tract following aerosol inhalation. *J Pharm Sci*, 1986. **75**: 433-438.

71. Wuerthwein, G., Rehder, S., and Rohdewald, P., Lipophilicity and receptor Affinity of glucocorticoids. *Pharm Ztg Wiss*, 1992. **137**: 161-165.

72. Loew, D., Schuster, O., and Graul, E.H., Dose-dependent pharmacokineitcs of dexamethasone. *Eur J Clin Pharmacol*, 1986. **30**: 225-230.

73. Rohatagi, S., Hochhaus, G., Moellmann, H., Barth, J., Galia, E., Erdmann, M., Sourgens, H., and Derendorf, H., Pharmacokinetic and Pharmacodynamic Evaluation of Triamcinolone Acetonide after Intravenous, Oral, and Inhaled Administration. *J Clin Pharmacol*, 1995. **35**(12): 1187-1193.

74. Ryrfeldt, A., Andersson, P., Edsbaecker, S., Tonnesson, M., Davies, D., and Pauwels, R., Pharmacokinetics and metabolism of budesonide, a selective glucocorticoid. *Eur J Respir Dis*, 1982. **63 (Suppl. 122)**: 86-95.

75. Rohatagi, S., Bye, A., Falcoz, C., Mackie, A.E., Meibohm, B., Moellmann, H., and Derendorf, H., Dynamic modeling of cortisol reduction after inhaled administration of fluticasone propionate. *J Clin Pharmacol*, 1996. **36**(10): 938-41.

76. Rohdewald, P., Moellmann, H., Barth, J., Rehder, J., and Derendorf, H., Pharmacokinetics of dexamethasone and its phosphate ester. *Biopharm Drug Dispos*, 1987. **8**(3): 205-12.

77. Chaplin, M.D., Rooks, W.d., Swenson, E.W., Cooper, W.C., Nerenberg, C., and Chu, N.I., Flunisolide metabolism and dynamics of a metabolite. *Clin Pharmacol Ther*, 1980. **27**(3): 402-13.

78. Derendorf, H., Hochhaus, G., Rohatagi, S., Moellmann, H., Barth, J., Sourgens, H., and Erdmann, M., Pharmacokinetics of triamcinolone acetonide after intravenous, oral, and inhaled administration. *J Clin Pharmacol*, 1995. **35**(3): 302-5.

79. Mackie, A.E., Ventresca, G.P., Fuller, R.W., and Bye, A., Pharmacokinetics of intravenous fluticasone proprionate in healthy volunteers. *Br J Clin Pharmacol*, 1996. **41**: 539-542.

80. Braat, M.C.P., Oosterhuis, B., Koopmans, R.P., Meewis, J.M., and VanBoxtel, C.J., Kinetic-dynamic modeling of lymphocytopenia induced by the combined action of dexamethasone and hydrocortisone in humans, after inhalation and intravenous administration of dexamethasone. *Journal of Pharmacology and Experimental Therapeutics*, 1992. **262**(2): 509-515.

81. Duggan, D.E., Yeh, K.C., Matalia, N., Ditzler, C.A., and McMahon, F.G., Bioavailability of oral dexamethasone. *Clin Pharmacol Ther*, 1975. **18**(2): 205-209.

82. Ventresca, G., Mackie, A., Moss, J., McDowall, J., and Bye, A., Absorption of oral fluticasone propionate in healthy subjects. *Am J Resp Crit Care Med*, 1994. **149**: A214.

83. Falcoz, C., Mackie, A., McDowall, J., McRae, J., Yogendran, L., Ventresca, G., and Bye, A., Oral bioavailability of fluticasone propionate in healthy subjects. *Brit J Clin Pharmacol*, 1996. **41**: 459P-60P.

84. Derendorf, H., Hochhaus, G., Rohatagi, S., Moellmann, H., Barth, J., and Erdmann, M., Oral and pulmonary bioavailability of triamcinolone acetonide. *J Clin Pharmacol*, 1995. **35**: 302-305.

85. Brattsand, R. and Axelsson, B.I., *Basis of airway selelctivity of inhaled glucocorticoids*, in *Inhaled glucocorticoids in asthma*, R.P. Schleimer, W.W. Busse, and P.M. O'Byrne, Editors. 1997, Marcel Dekker, New York: 351-379.

86. Brown, R.A., Jr. and Schanker, L.S., Absorption of aerosolized drugs from the rat lung. *Drug Metab Dispos*, 1983. **11**(4): 355-60.

87. Burton, J.A. and Schanker, L.S., Absorption of corticosteroids from the rat lung. *Steroids*, 1974. **23**: 617-624.

88. Moellmann, H., et al., Pharmacokinetic/pharmacodynamic evaluation of systemic effects of flunisolide after inhalation. *J Clin Pharmacol*, 1997. **37**(10): 893-903.

89. Rohatagi, S., Hochhaus, G., Moellmann, H., Barth, J., Galia, E., Erdmann, M., Sourgens, H., and Derendorf, H., Pharmacokinetic and pharmacodynamic evaluation of triamcinolone acetonide after intravenous, oral, and inhaled administration. *J Clin Pharmacol*, 1995. **35**(12): 1187-93.

90. Moellmann, H., et al., Pharmacokinetic and pharmacodynamic evaluation of fluticasone propionate after inhaled administration. *Eur J Clin Pharmacol*, 1998. **53**(6): 459-67.

91. Falcoz, C., Brindley, C., Mackie, A., and Bye, A., Input Rate into the systemic Circulation of fluticasone propionate after a 1000 μg inhaled dose from the diskhaler. *J Clin Pharmacol*, 1996. **35**: 927.

92. Moellmann, H., Hochhaus, G., Rohatagi, S., Barth, J., Derendorf, H., Krieg, M., Weisser, H., and Moellmann, A.C., Pharmacokinetics and pharmacodynamics of cloprednol. *Int J Clin Pharmacol Ther*, 1996. **34**(1): 1-5.

93. Thorsson, L., Dahlstrom, K., Edsbaecker, S., Kallen, A., Paulson, J., and Wiren, J.E., Pharmacokinetics and systemic effects of inhaled fluticasone propionate in healthy subjects. *Br J Clin Pharmacol*, 1997. **43**(2): 155-61.

94. Sergeev, P.V., Kalinin, G.V., and Dukhanin, A.S., Plasma membrane of thymocytes - home of specific glucocorticoid binding sites. *Biull Eksp Biol Med*, 1986. **102**(8): 192-4.

95. Allera, A. and Wildt, L., Glucocorticoid-recognizing and -effector sites in rat liver plasma membrane. Kinetics of corticosterone uptake by isolated membrane vesicles - II. Comparative influx and efflux. *J Steroid Biochem Mol Biol*, 1992. **42**(7): 757-71.

96. Lackner, C., Daufeldt, S., Wildt, L., and Allera, A., Glucocorticoid-recognizing and -effector sites in rat liver plasma membrane. Kinetics of corticosterone uptake by isolated membrane vesicles. III. Specificity and stereospecificity. *J Steroid Biochem Mol Biol*, 1998. **64**(1-2): 69-82.

97. Meijer, O.C., de Lange, E.C., Breimer, D.D., de Boer, A.G., Workel, J.O., and de Kloet, E.R., Penetration of dexamethasone into brain glucocorticoid targets is enhanced in mdr1A P-glycoprotein knockout mice. *Endocrinology*, 1998. **139**(4): 1789-93.

98. Schinkel, A.H., Wagenaar, E., van Deemter, L., Mol, C.A., and Borst, P., Absence of the mdr1a P-Glycoprotein in mice affects tissue distribution and pharmacokinetics of dexamethasone, digoxin, and cyclosporin A. *J Clin Invest*, 1995. **96**(4): 1698-705.

99. Rocci, M.L., D'Ambrosio, R., Johnson, N.F., and Jusko, W.J., Prednisolone Binding to Albumin and Transcortin in the Presence of Cortisol. *Biochem Pharmacol*, 1982. **31**(3): 289-292.

100. Milsap, R.L. and Jusko, w.J., Binding of prednisolone to a1-acid glycoprotein. *J Ster Biochem*, 1983. **18**(2): 191-194.

101. Esmailpour, N., Hogger, P., Rabe, K.F., Heitmann, U., Nakashima, M., and Rohdewald, P., Distribution of inhaled fluticasone propionate between human lung tissue and serum in vivo. *Eur Respir J*, 1997. **10**(7): 1496-9.

102. Tunek, A., Sjodin, K., and Hallstrom, G., Reversible formation of fatty acid esters of budesonide, an antiasthma glucocorticoid, in human lung and liver microsomes. *Drug Metab Dispos*, 1997. **25**(11): 1311-7.

103. Rohdewald, P., Moellmann, H., Mueller, K.M., and Hochhaus, G., *Glucocorticoid receptors in the respiration tract*. Bochumer Treff 1984, Rezeptoren und nervoese Versorgung des bronchopulmonalen Systems. 1985, Munich: Verlag Gedon & Reuss. 223-242.

104. Jonsson, G., Astrom, A., and Andersson, P., Budesonide is metabolized by cytochrome P450 3A (CYP3A) enzymes in human liver. *Drug Metab Dispos*, 1995. **23**(1): 137-42.

105. Shaw, R.J., Pharmacology of fluticasone propionate. *Respir Med*, 1994. **88 Suppl A**: 5-8.

106. Edsbaecker, S., Andersson, P., Lindberg, C., Paulson, J., Ryrfeldt, A., and Thalen, A., Liver metabolism of budesonide in rat, mouse, and man. *Drug Met Disp*, 1987. **15**(3): 403-411.

107. Glaxo-Wellcome, I., *FLOVENT Product Information,*. 1996, Research Triangle Park, NC, USA.

108. Wolff, M.E., Baxter, J.D., Kollmann, P.A., and Lee, D.L., Nature of Steroid-Glucocorticoid Receptor Interactions: Thermodynamic Analysis of the Binding Reaction. *Biochemistry*, 1978. **17**: 3201-3207.

109. Huang, M.-J., Tamada, S., Hochhaus, G., and Bodor, N. An AM1-based model for the estimation of the relative binding affinity for glucocorticoids. in *1st Drug Optimization via Retrometabolism Conference*. 1997. Amelia Island: Die Pharmazie.

110. Hochhaus, G., Druzgala, P., Hochhaus, R., Huang, M.-J., and Bodor, N., Glucocorticoid activity and structure activity relationships in a series of some novel 17 a-ether-substituted steroids: influence of 17a-substituents. *Drug Des Del*, 1991. **8**: 117-125.

111. Druzgala, P., Hochhaus, G., and Bodor, N., Soft drugs--10. Blanching activity and receptor binding affinity of a new type of glucocorticoid: loteprednol etabonate. *J Ster Biochem Mol Biol*, 1991. **38**(2): 149-54.

112. Dahlberg, E., Thalen, A., Brattsand, R., Gustafsson, J.A., Johansson, U., Roempke, K., and Saatok, T., Correlation between chemical structure, receptor binding, and biological activity of some novel, high active, 16a, 17a acetal substituted glucocorticoids. *Mol Pharmacol*, 1984. **25**: 70-78.

113. Rohdewald, P., Moellmann, H., and Hochhaus, G., Receptor binding affinities of commercial glucocorticoids to the glucocorticoid receptor of human lung. *Atemw-Lungenhrkh*, 1984. **10**: 484-487.

114. Hoegger, P. and Rohdewald, P., Binding kinetics of fluticasone propionate to the human glucocorticoid receptor. *Steroids*, 1994. **59**: 597-602.

115. Wuerthwein, G., Rehder, S., and Rohdewald, P., Lipophilicity and receptor affinity of glucocorticoids. *Pharm Ztg Wiss*, 1992. **137**(4): 161-167.

116. Druzgala, P., Hochhaus, G., and Bodor, N., Soft drugs 10: Blanching activity and receptor binding affinity of a new type of glucocorticoid: loteprednol etabonate. *J Steroid Biochem*, 1991. **38**(2): 149-154.

117. Derendorf, H., Hochhaus, G., Moellmann, H., Barth, J., Krieg, M., Tunn, S., and Mollmann, C., Receptor-based pharmacokinetic-pharmacodynamic analysis of corticosteroids. *J Clin Pharmacol*, 1993. **33**(2): 115-23.

118. Hoegger, P. and Rohdewald, P., Glucocorticoid receptors and fluticasone propionate. *Rev Cont Pharmacother*, 1998. **9**(8): 501-519.

119. Dahlberg, E., Thalen, A., Brattsand, R., Gustafsson, J.-A., Johansson, U., Roemke, K., and Saartrok, T., Correlation between chemical structure, Receptor binding, and biological activity of some novel, highly active, 16a,17a- acetal- substituted-glucocorticoids. *Mol Pharmacol*, 1984. **25**: 70-78.

120. Hochhaus, G., Rohdewald, P., Moellmann, H., and Grechuchna, D., Identification of glucocorticoid receptors in normal and neoplastic human lungs. *Resp Exp Med*, 1983. **182**: 71-78.

121. Beato, M., Rousseau, G.G., and Feigelson, P., Correlation between glucocorticoid binding to specific liver cytosol receptors and enzyme induction. *Biochem Biophys Res Commun*, 1972. **47**: 1464-1472.

122. Edsbaecker, S. and Jendro, M., *Modes to achieve topical selectivity of inhaled glucocorticoids-focus on budesonide*, in *Respiratory Drug Delivery VI*, R.N. Dalby, P.R. Byron, and S.J. Farr, Editors. 1998, Interpharm Press, Inc., Buffalo Grove, IL: 71-82.

123. Kelly, H.W., Comparison of inhaled corticosteroids. *Ann Pharmacother*, 1998. **32**(2): 220-32.

124. Moellmann, H., Rohdewald, P., Schmidt, E.W., and Derendorf, H., Pharmacokinetics of triamcinolone acetonide and its phosphate ester. *Eur J Clin Pharmacol*, 1985. **29**: 85-89.

125. Suarez, S., Gonzalez-Rothi, R., Schreier, H., and Hochhaus, G., The effect of dose and release rate on pulmonary targeting of of liposomal triamcinolone acetonide phosphate. *Pharm Res*, 1998. **15**(3): 461-465.

126. Astra-USA, Budesonide Inhalation powder:200 and 400 mg/dose (Pulmicort Turbohaler) NDA 20-441. *Clin Pharmacol Biopharm Rev*, 1997: 1-51.

127. Chanoine, F., Grenot, C., Heidmann, P., and Junien, J.L., Pharmacokinetics of butixocort 21-propionate, budesonide, and beclomethasone dipropionate in the rat after intratracheal, intravenous, and oral treatments. *Drug Metab Dispos*, 1991. **19**(2): 546-53.

128. Ryrfeldt, A., Persson, G., and Nilsson, E., Pulmonary disposition of the potent glucocorticoid budesonide, evaluated in an isolated perfused rat lung model. *Biochem Pharmacol*, 1989. **38**(1): 17-22.

129. Meibohm, B., Moellmann, H., Wagner, M., Hochhaus, G., Moellmann, A., and Derendorf, H., The Clinical Pharmacology of Fluticasone Propionate. *Rev Contemp Pharmacother*, 1998. **9**(8): 535-549.

130. Andersson, P., Brattsand, R., Dahlstroem, K., and Edsbaecker, S., Oral availability of fluticasone propionate. *Br J Clin Pharmac*, 1993. **36**: 135-136.

131. Derendorf, H., Pharmacokinetic and pharmacodynamic properties of inhaled corticosteroids in relation to efficacy and safety. *Respir Med*, 1997. **91 Suppl A**: 22-8.

132. Farr, S.J., Kellaway, I.W., and B., C.-M., Comparison of solute partitioning and efflux of liposomes formed by a conventional and aerosolized method. *Int J Pharmaceut*, 1989. **51**: 39-46.

133. Schreier, H., Lukyanov, A.N., Hochhaus, G., and R.J., G.R., Thermodynamic and kinetic aspects of the interaction of triamcinolone acetonide with liposomes. *Proceed Intern Symp Control Rel Bioact Mater*, 1994. **21**: 228-229.

134. Goundalkar, A. and Mezei, M., Chemical modification of triamcinolone acetonide to improve liposomal encapsulation. *J Pharm Sci*, 1983. **73**(6): 834-5.

135. Shaw, I.H., Liposomal retention of a modified anti-inflammatory steroid. *Biochem J*, 1976. **158**: 473-76.

136. Therin, M., Christel, P., Li, S., Garreau, H., and Vert, M., In vivo degradation of massive poly(alpha-hydroxy acids): validation of in vitro findings. *Biomaterials*, 1992. **13**(9): 594-600.

137. Chu, C.R., Monosov, A.Z., and Amiel, D., In situ assessment of cell viability within biodegradable polylactic acid polymer matrices. *Biomaterials*, 1995. **16**(18): 1381-4.

138. Lai, Y.L., Mehta, R.C., Thacker, A.A., Yoo, S.D., McNamara, P.J., and DeLuca, P.P., Sustained bronchodilation with isoproterenol poly(glycolide-co-lactide) microspheres. *Pharm Res*, 1993. **10**(1): 119-25.

139. Hickey, A., Suarez, S., Bhat, M., O'hara, P., Lalor, C., Atkins, K., Hopfer, R., and McMurray, D. Efficacy of rifampicin-poly(lactide-co-glycolide) microspheres in treating tuberculosis. in *Respiratory Drug Delivery VI*. 1998. Hilton Head, SC: Interpharm Press, Inc.

140. Thies, C., Microcapsules as drug delivery devices. *Crit Rev Biomed Eng*, 1982. **8**(4): 335-83.

141. Manekar, N.C., Puranik, P.K., and Joshi, S.B., Microencapsulation of propranolol hydrochloride by the solvent evaporation technique. *J Microencapsul*, 1992. **9**(1): 63-6.

142. Conti, B., Pavanetto, F., and Genta, I., Use of polylactic acid for the preparation of microparticulate drug delivery systems. *J Microencapsul*, 1992. **9**(2): 153-66.

143. Gopferich, A., Alonso, M.J., and Langer, R., Development and characterization of microencapsulated microspheres. *Pharm Res*, 1994. **11**(11): 1568-74.

144. Kawashima, Y., Serigano, T., Hino, T., Yamamoto, H., and Takeuchi, H., A new powder design method to improve inhalation efficiency of pranlukast hydrate dry powder aerosols by surface modification with hydroxypropylmethylcellulose phthalate nanospheres. *Pharm Res*, 1998. **15**(11): 1748-52.

145. Glatt, Multi-purpose Fluid Bed Processing. *Product Literature*, 1998.

146. Fitz-Gerald, J., Synthesis and Characterization of Engineered Particulates with Controlled Surface Architecture. *PhD Dissertation*, 1998.

147. Hansen, S. and Robitaille, T., Formation of polymer films by pulsed laser evaporation. *Applied Physics Letters*, 1988. **52**(1): 81-83.

148. Blanchet, G., Fincher, C., Jackson, C., Shah, S., and Gardner, K., Laser ablation and the production of polymer films. *Science*, 1993. **262**: 719-721.

149. Li, S., Arenholz, E., Heitz, J., and Bauerle, D., Pulsed-laser deposition of crystalline Teflon (PTFE) films. *App Surf Sci*, 1998. **125**: 17-22.

150. Suzuki, M., Nakata, Y., Nagai, H., Goto, K., Nishimura, O., and Okutani, T., Synthesis of silicon-based polymer films by UV laser ablation deposition of poly(methylphenylsilane). *Mat Sci Eng A*, 1998. **246**: 36-44.

151. Suarez, S., Biopharmaceutical Aspects Relevant to Pulmonary Targeting of Inhaled Glucocorticoids: Application to Liposomes and Dry-Powders. *PhD Dissertation*, 1997.

152. Shah, V.P., Konecny, J.J., Everett, R.L., McCullough, B., Noorizadeh, A.C., and Skelly, J.P., In vitro dissolution profile of water-insoluble drug dosage forms in the presence of surfactants. *Pharm Res*, 1989. **6**(7): 612-8.

153. FDA, SUPAC-MR: Modified Release Solid Oral Dosage Forms Guidelines, . 1998, Food and Drug Administration, Washington, D.C.

154. Li, Y.N., Tattam, B., Brown, K.F., and Seale, J.P., Determination of epimers 22R and 22S of budesonide in human plasma by high-performance liquid chromatography-atmospheric pressure chemical ionization mass spectrometry. *J Chromatogr B Biomed Appl*, 1996. **683**(2): 259-68.

155. Krishnaswami, S., Moellmann, H., Derendorf, H., and Hochhaus, G., A sensitive APCI MRM LC/MS method for the quantification of fluticasone propionate in human plasma. *Pharm Res*, 1999. **Submitted**.

156. Gibaldi, M. and Perrier, D., *Pharmacokinetics*. 2nd ed. 1982, New York: Marcel Dekker , Inc.

157. Burton, J.A. and Schanker, L.S., Absorption of corticosteroids from the rat lung. *Steroids*, 1974. **23**(5): 617-24.

158. Davies, B. and Morris, T., Physiological parameters in laboratory animals and humans [editorial]. *Pharm Res*, 1993. **10**(7): 1093-5.

159. Derendorf, H., Moellmann, H., Hochhaus, G., Meibohm, B., and Barth, J., Clinical PK/PD modeling as a tool in drug development of corticosteroids. *Int J Clin Pharmacol Ther*, 1997. **35**: 481-488.

160. Hochhaus, G., Gonzales-Rothi, R., Lukyanov, A., Derendorf, H., Schreier, H., and Dalla Costa, T., Assessment of glucocorticoid lung targeting by ex-vivo receptor binding studies. *Pharm Res*, 1995. **12**: 134-137.

161. Brattsand, R., Thalen, A., Roempke, K., Kaellstroem, L., and Gruvstad, E., Influence of 16a,17a-acetal substitution and steroid nucleus fluorination on the topical to systemic ratio of glucocorticoid. *J Steroid Biochem*, 1982. **16**: 779-786.

162. Hochhaus, G., Binding affinities of commercially available glucocorticoids to the glucocorticoid receptor of the human lung, in *Institute of Pharmaceutical Chemistry*. 1983, Westfaelische Wilhelms Universitaet, Muenster.

163. Rohdewald, P., Moellmann, H.W., and Hochhaus, G., Affinities of glucocorticoids for glucocorticoid receptors in the human lung. *Agents and Actions*, 1985. **17**(3/4): 290-291.

164. Reul, J., van den Bosch, F., and de Kloet, E., Relative occupation of type-I and type-II corticosteroid receptors in rat brain following stress and dexamethasone treatment: functional implications. *J Endocr*, 1987. **115**: 459-467.

165. Bloemena, E., Weinreich, S., and Schellekens, P.T.A., The influence of prednisolone on the recirculation of peripheral blood lymphocytes in vivo. *Clin Exp Imm*, 1990. **80**: 460-466.

166. Miller, A.H., Spencer, R.L., Pearce, B.D., Pisell, T.L., Azrieli, Y., Tanapat, P., Moday, H., Rhee, R., and McEwen, B.S.,

Glucocorticoid receptors are differentially expressed in the cells and tissues of the immune system. *Cell Immunol*, 1998. **186**(1): 45-54.

167. Brattsand, R. and Selroos, O., *Current drugs for respiratory diseases.* Drugs and the lung, ed. C.P. Page and W.J. Metzger. 1994, New York: Raven, Press. 42-110.

168. Chrisey, D. and Hubler, G., Pulsed Laser Deposition of Thin Films. 1994. **1**: 200.

169. Hrkach, J.S., Peracchia, M.T., Domb, A., Lotan, N., and Langer, R., Nanotechnology for biomaterials engineering: structural characterization of amphiphilic polymeric nanoparticles by 1H NMR spectroscopy. *Biomaterials*, 1997. **18**(1): 27-30.

170. Kreitz, M.R., Domm, J.A., and Mathiowitz, E., Controlled delivery of therapeutics from microporous membranes. II. In vitro degradation and release of heparin-loaded poly(D,L-lactide-co- glycolide). *Biomaterials*, 1997. **18**(24): 1645-51.

171. Witschi, C. and Mrsny, R.J., In vitro evaluation of microparticles and polymer gels for use as nasal platforms for protein delivery [In Process Citation]. *Pharm Res*, 1999. **16**(3): 382-90.

172. Pillai, R.S., Yeates, D.B., Miller, I.F., and Hickey, A.J., Controlled dissolution from wax-coated aerosol particles in canine lungs. *J Appl Physiol*, 1998. **84**(2): 717-25.

173. Fielding, R.M. and Abra, R.M., Factors affecting the release rate of terbutaline from liposome formulations after intratracheal instillation in the guinea pig. *Pharm Res*, 1992. **9**(2): 220-3.

174. McCullough, H.N. and Juliano, R.L., Organ-selective action of an antitumor drug: pharmacologic studies of liposome-encapsulated beta-cytosine arabinoside administered via the respiratory system of the rat. *J Natl Cancer Inst*, 1979. **63**(3): 727-31.

## BIOGRAPHICAL SKETCH

James David Talton was born on January 24, 1971, in Fort Lauderdale, Florida. He graduated from Plantation High School in 1988. He entered the University of Florida summer of 1988, after spending the summer before at UF in the Summer Science Training Program. He completed his B.S. and M.S. in materials science and engineering in 1993 and 1995, respectively. He entered the pharmaceutics program at the University of Florida in fall 1995. He attended an internship at Boehringer Ingelheim Pharmaceutics in Ridgefield, Conneticut, during the summer of 1996. He completed his graduate work under the supervision of Dr. Guenther Hochhaus, receiving his Ph.D. in pharmaceutics in August 1999.

I certify that I have read this study and that in my opinion it conforms to acceptable standards of scholarly presentation and is fully adequate, in scope and quality, as a dissertation for the degree of Doctor of Philosophy.

Guenther Hochhaus, Chair
Associate Professor of
Pharmaceutics

I certify that I have read this study and that in my opinion it conforms to acceptable standards of scholarly presentation and is fully adequate, in scope and quality, as a dissertation for the degree of Doctor of Philosophy.

Hartmut Derendorf
Professor of Pharmaceutics

I certify that I have read this study and that in my opinion it conforms to acceptable standards of scholarly presentation and is fully adequate, in scope and quality, as a dissertation for the degree of Doctor of Philosophy.

Jeffrey Hughes
Assistant Professor of Pharmaceutics

I certify that I have read this study and that in my opinion it conforms to acceptable standards of scholarly presentation and is fully adequate, in scope and quality, as a dissertation for the degree of Doctor of Philosophy.

Gayle Brazeau
Associate Professor of
Pharmaceutics

I certify that I have read this study and that in my opinion it conforms to acceptable standards of scholarly presentation and is fully adequate, in scope and quality, as a dissertation for the degree of Doctor of Philosophy.

Christopher Batich
Professor of Materials Science and
Engineering

This dissertation was submitted to the Graduate Faculty of the College of Pharmacy and to the Graduate School and was accepted as partial fulfillment of the requirements for the degree of Doctor of Philosophy.

August 1999

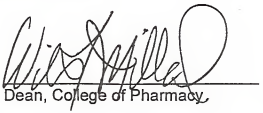

Dean, College of Pharmacy

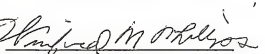

Dean, Graduate School